

# **Teardown Evaluation of Areas of Interest From the T-34A N141SW Aircraft Wreckage**

March 2006

DOT/FAA/AR-TN05/57

This document is available to the public through the National Technical Information Service (NTIS), Springfield, Virginia 22161.



U.S. Department of Transportation  
**Federal Aviation Administration**

## **NOTICE**

This document is disseminated under the sponsorship of the U.S. Department of Transportation in the interest of information exchange. The United States Government assumes no liability for the contents or use thereof. The United States Government does not endorse products or manufacturers. Trade or manufacturer's names appear herein solely because they are considered essential to the objective of this report. This document does not constitute FAA certification policy. Consult your local FAA aircraft certification office as to its use.

This report is available at the Federal Aviation Administration William J. Hughes Technical Center's Full-Text Technical Reports page: [actlibrary.tc.faa.gov](http://actlibrary.tc.faa.gov) in Adobe Acrobat portable document format (PDF).

1. Report No. <b>DOT/FAA/AR-TN05/57</b>		2. Government Accession No.		3. Recipient's Catalog No.	
4. Title and Subtitle <b>TEARDOWN EVALUATION OF AREAS OF INTEREST FROM THE T-34A N141SW AIRCRAFT WRECKAGE</b>				5. Report Date <b>March 2006</b>	
				6. Performing Organization Code	
7. Author(s) <b>Melinda Laubach and Dale Cope</b>				8. Performing Organization Report No.	
9. Performing Organization Name and Address <b>National Institute for Aviation Research Wichita State University 1845 Fairmount Wichita, Kansas 67260</b>				10. Work Unit No. (TRAIS)	
				11. Contract or Grant No. <b>01-C-AW-WISU</b>	
12. Sponsoring Agency Name and Address <b>U.S. Department of Transportation Federal Aviation Administration Office of Aviation Research and Development Washington, DC 20591</b>				13. Type of Report and Period Covered <b>Technical Note</b>	
				14. Sponsoring Agency Code <b>ACE-113</b>	
15. Supplementary Notes <b>The Federal Aviation Administration Airport and Aircraft Safety R&amp;D Division COTR was Michael Shiao.</b>					
16. Abstract <p>To aid with the assessment of aging acrobatic aircraft, the Federal Aviation Administration (FAA) teamed with the National Institute for Aviation Research of Wichita State University to teardown and inspect areas of interest from the T-34A N141SW accident aircraft. Due to the recent history of fatigue cracking and failure, a destructive evaluation of the T-34A would be useful to the FAA to specifically address the T-34A concerns, and in a general sense, to assess the condition of a high-time acrobatic category aircraft. The following four areas of interest from the N141SW accident aircraft were examined for cracks and corrosion: right wing front carry-through lower spar, horizontal and vertical stabilizer attachment points, right wing rear spar lower cap wing station 66, and right wing rear spar lower bathtub fitting. Cracks found on these areas of the accident aircraft were opened, and the crack faces were analyzed to determine failure mode. Surrounding structure was also inspected microscopically for additional defects.</p>					
17. Key Words <b>Aging, Teardown, Fatigue, Nondestructive evaluation</b>			18. Distribution Statement <b>This document is available to the public through the National Technical Information Service (NTIS), Springfield, Virginia 22161.</b>		
19. Security Classif. (of this report) <b>Unclassified</b>		20. Security Classif. (of this page) <b>Unclassified</b>		21. No. of Pages <b>60</b>	
				22. Price	

## TABLE OF CONTENTS

	Page
EXECUTIVE SUMMARY	xi
1. INTRODUCTION	1
2. TEARDOWN EVALUATION	3
2.1 Surface Eddy-Current Nondestructive Inspection	4
2.2 Disassembly Phase	4
2.3 Microscopic Examination	7
2.3.1 Right Wing Front Carry-Through	7
2.3.2 Vertical and Horizontal Stabilizer Attachment Points	29
2.3.3 Right Wing Rear Spar WS 66	42
2.3.4 Right Wing Rear Spar Bathtub Fitting	46
3. SUMMARY OF FINDINGS	46



## LIST OF FIGURES

Figure	Page
1 Typical T-34A Aircraft	2
2 Wreckage as Received	3
3 Aft Side of the Right Wing Front Carry-Through Outer (-33) Channel, Cracks 9 and 10	4
4 Right Wing Front Carry-Through Lower Spar	5
5 Horizontal and Vertical Stabilizer Attachment Points	5
6 Right Wing Rear Spar WS 66	6
7 Right Wing Rear Spar Lower Bathtub Fitting	6
8 Right Wing Front Carry-Through Stackup	7
9 Locations of Cracks 1 and 2 on the Right Wing Front Carry-Through Middle (-31) Channel Forward Side	8
10 Crack 1 Fracture Face	9
11 Crack 2 Fracture Face	9
12 Locations of Cracks 3 and 4 on the Right Wing Front Carry-Through Middle (-31) Channel Aft Side	10
13 Crack 3 Fracture Face	11
14 Crack 4 Fracture Face	11
15 Locations of Cracks 5 and 6 on the Right Wing Front Carry-Through Middle (-31) Channel Lower Surface	12
16 Crack 5 Fracture Face	13
17 Locations of Cracks 7 and 8 on the Right Wing Front Carry-Through Outer (-33) Channel Forward Side	14
18 Crack 8 Fracture Face	14
19 Surface Face SEM Fractograph of Crack 8	15
20 Locations of Cracks 9 and 10 on the Right Wing Front Carry-Through Outer (-33) Channel Aft Side	16

21	Crack 10 Fracture Face	16
22	Surface Face SEM Fractograph of Crack 10	17
23	Locations of Cracks 11 and 12 on the Right Wing Front Carry-Through Outer (-33) Channel Lower Surface	18
24	Crack 12 Fracture Face	18
25	Surface Face SEM Fractograph of Crack 12 (X3,300)	19
26	Surface Face SEM Fractograph of Crack 12 (X2,000)	19
27	Right Wing Front Carry-Through Aft Side Stackup	20
28	Locations of Cracks 13, 14, and 15 on the Right Wing Front Carry-Through Middle Layer Aft Side Web Skin	21
29	Crack 13 Fracture Face	21
30	Crack 14 Fracture Face	22
31	Locations of Cracks 16 and 17 on the Right Wing Front Carry-Through Middle Layer Aft Side Web Skin	22
32	Locations of Cracks 18-22 on the Right Wing Front Spar Carry-Through Middle Layer Aft Side Web Skin	23
33	Detailed Locations of Cracks 18-22 on the Right Wing Front Spar Carry-Through Middle Layer Aft Side Web Skin	24
34	Crack 18 Fracture Face	24
35	Crack 19 Fracture Face	25
36	Crack 20 Fracture Face	25
37	Crack 21 Fracture Face	26
38	Right Wing Front Carry-Through Forward Side Stackup	27
39	Location of Crack 23 on the Right Wing Front Carry-Through Middle Layer Forward Side Web Skin	27
40	Locations of Cracks 24 and 25 on the Right Wing Front Carry-Through Middle Layer Forward Side Web Skin	28
41	Crack 24 Fracture Face	28

42	Location of Crack 26 in the Vertical Stabilizer Bulkhead Top Layer	29
43	Crack 26 in the Vertical Stabilizer Bulkhead Top Layer	30
44	Locations of Cracks 27 and 28 in the Vertical Stabilizer Bulkhead Middle Layer	31
45	Crack 27 in the Vertical Stabilizer Bulkhead Middle Layer	32
46	Crack 28 in the Vertical Stabilizer Bulkhead Middle Layer	32
47	Crack 28 in the Vertical Stabilizer Bulkhead Middle Layer During the Fluorescent Liquid Penetrant Inspection	33
48	Crack 29 in the Vertical Stabilizer Bulkhead Bottom Layer	34
49	Crack 29 in the Vertical Stabilizer Bulkhead Bottom Layer During the Fluorescent Liquid Penetrant Inspection	34
50	Locations of Cracks 30, 31, and 32 in the Horizontal Stabilizer Bulkhead Top Layer	35
51	Crack 30 in the Horizontal Stabilizer Bulkhead Top Layer	35
52	Crack 30 in the Horizontal Stabilizer Bulkhead Top Layer Under Ultraviolet Light	36
53	Crack 31 in the Horizontal Stabilizer Bulkhead Top Layer	36
54	Crack 31 in the Horizontal Stabilizer Bulkhead Top Layer During the Fluorescent Liquid Penetrant Inspection	37
55	Crack 32 in the Horizontal Stabilizer Bulkhead Top Layer	37
56	Crack 32 in the Horizontal Stabilizer Bulkhead Top Layer Under Ultraviolet Light	38
57	Locations of Cracks 33, 34, and 35 in the Horizontal Stabilizer Bulkhead Middle Layer	39
58	Crack 33 in the Horizontal Stabilizer Bulkhead Middle Layer	39
59	Crack 33 in the Horizontal Stabilizer Bulkhead Middle Layer During the Fluorescent Liquid Penetrant Inspection	40
60	Crack 34 in the Horizontal Stabilizer Bulkhead Middle Layer	40
61	Crack 34 in the Horizontal Stabilizer Bulkhead Middle Layer Under Ultraviolet Light	41

62	Crack 35 in the Horizontal Stabilizer Bulkhead Middle Layer	41
63	Crack 35 in the Horizontal Stabilizer Bulkhead Middle Layer During the Fluorescent Liquid Penetrant Inspection	42
64	Overview of Crack Locations at WS 66	43
65	Cracks 36 and 37 on Right Wing Rear Spar WS 66	43
66	Crack 36 Fracture Face	44
67	Surface Face Sem Fractograph of Crack 36	44
68	Crack 37 Fracture Face	45
69	Surface Face SEM Fractograph of Crack 37	45
70	Right Wing Rear Spar Lower Bathtub Fitting	46

## LIST OF TABLES

Table		Page
1	Summary of Findings for T-34A Accident Aircraft	47

## LIST OF ACRONYMS

AD	Airworthiness Directive
FAA	Federal Aviation Administration
NIAR	National Institute for Aviation Research
NTSB	National Transportation Safety Board
SEM	Scanning electron microscope
WS	Wing Station

## EXECUTIVE SUMMARY

To aid with the assessment of aging acrobatic aircraft, the Federal Aviation Administration (FAA) teamed with the National Institute for Aviation Research of Wichita State University to teardown and inspect four areas of interest from the T-34A N141SW accident aircraft, which was obtained through the FAA after the accident investigation by the National Transportation Safety Board. Due to the recent history of fatigue cracking and failure, a destructive evaluation of the T-34A would be useful to the FAA for specifically addressing T-34A concerns, and in a general sense, assessing the condition of a high-time acrobatic category aircraft. The following four areas from the N141SW accident aircraft were examined for cracks and corrosion: right wing front carry-through lower spar, horizontal and vertical stabilizer attachment points, right wing rear spar lower cap wing station (WS) 66, and right wing rear spar lower bathtub fitting. Cracks found on these areas of the aircraft were opened, and the crack faces were analyzed to determine failure mode. Surrounding structure was also inspected microscopically for additional defects.

During the destructive evaluation, a total of 25 cracks were found on the right wing front carry-through lower spar, 10 cracks were located on the horizontal and vertical stabilizer attachment points, 2 cracks occurred on the right wing rear spar lower cap, and 1 crack was found in the right wing rear spar lower bathtub fitting. In the carry-through structure, three cracks, ranging in size from 0.15 to 5.28 inches, were caused solely by overload. Sixteen cracks had fatigue origins with fatigue lengths ranging from 0.05 to 0.53 inch. These sixteen cracks then extended due to overload conditions. The cause of failure could not be determined in the other six cracks, which ranged in length from 0.10 to 1.17 inches. Four cracks, ranging from 0.28 to 1.4 inches, were found on the vertical stabilizer bulkhead with the failure mode being overload. Six cracks due solely to overload were found on the horizontal stabilizer bulkhead, which ranged in length from 0.13 to 1.13 inches. Two 1.187-inch-long cracks were found on the right wing rear spar at WS 66. Due to extensive metal smearing on the fracture faces, the cause of failure for these cracks could not be determined. Another crack, measuring 3.29 inches, was found on the right wing rear spar lower bathtub fitting. It was evident that the failure mode of this crack was not fatigue; however, the failure mode could not be conclusively determined.

## 1. INTRODUCTION.

The Beech Model T-34A was built in the 1950s and 1960s for the U.S. Navy and Air Force as military trainers. Although the military used the designation T-34A, the airplanes are designated as Model A45 on the Federal Aviation Administration (FAA) Type Certificate. The more common designation of T-34A is used in this report.

On April 19, 1999, a Beech T-34A, tail number N140SW, collided with the ground following the in-flight separation of the right wing near Rydal, Georgia. The aircraft entered a spiral and impacted the ground resulting in two fatal injuries. The examination of the airplane disclosed fatigue cracking in the spar material. The National Transportation Safety Board (NTSB) determined that the probable cause of this accident, accident investigation number ATL99FA072, was as follows: “Fracture of the wing spar as a result of fatigue cracking that occurred over an unknown number of flights and flight hours with a wing loading spectrum not anticipated during the design of the airplane.” The failures were located on the front spar lower cap at wing station (WS) 34 and on the rear spar lower cap at WS 66. The failures were caused by metal fatigue.

Following this accident, the FAA issued an Airworthiness Directive (AD) 99-12-02, which limited the maximum speed to 175 miles per hour and the flight envelope from +6/-3 g's to +2.5/-0 g's in an effort to prevent future overload failures in the vicinity of pre-existing fatigue cracks. AD 2001-13-18 was also issued to inspect critical areas for fatigue cracks on the front and rear spars per Raytheon Service Bulletin 57-3329. This AD required the bolthole eddy-current inspection of nine fasteners on the front spar at WS 34, one fastener site on the front spar at WS 64, and two fastener locations on the rear spar at WS 66. This AD also required the eddy-current inspection of the rear spar lower bathtub fittings.

On November 19, 2003, another in-flight breakup occurred involving a T-34A near Montgomery, Texas. While maneuvering in a simulated air-to-air combat scenario with another aircraft, the accident aircraft, registration number N44KK, was in a climbing right turn when the right wing separated from the aircraft. Subsequently, the aircraft spun uncontrolled to the ground, resulting in two fatalities. Examination of the separated wing revealed extensive fatigue cracking in both the front and rear spars. The NTSB determined that the probable causes of this accident, accident investigation number FTW04FA025, were as follows: “The non-compliance with applicable Airworthiness Directive, which required wing spar inspections, and the continued operation of the aircraft beyond the compliance time extension granted and per the approved Alternate Means of Compliance (AMOC). Also causal was the operation of the aircraft outside of its flight “G” load limitations.”

On December 7, 2004, a T-34A single-engine airplane, tail number N141SW, was destroyed when it impacted terrain following an in-flight separation of the left wing and subsequent loss of control near Montgomery, Texas. The airline transport pilot and pilot-rated passenger were both fatally injured. A review of maintenance records showed that the accident airplane was in compliance with AD 2001-13-18 R1, which the FAA issued as a result of an accident near Montgomery, Texas, in November 2003. Examination of the wreckage revealed the left wing forward spar carry-through structure failed about 6 inches inboard of the forward wing



attachment point, and the aft spar failed about 4 inches outboard of the aft wing attachment point. In addition, the investigation of accident investigation number DEN05FA032 revealed visual evidence of fatigue in locations not previously addressed by AD 2001-13-18 R1.

On December 10, 2004, the FAA issued an Emergency Airworthiness Directive, AD 2004-25-51, to address the preliminary findings of the investigation. According to this AD, the owners/operators had 10 hours time-in-service, and no later than 30 days after receipt of the emergency AD to return/position the airplane to a home base, hangar, maintenance facility, etc., until further action was determined by the FAA.

To aid with the assessment of aging acrobatic aircraft, the FAA contracted with the Aging Aircraft Research Laboratory at the National Institute for Aviation Research (NIAR) to teardown and inspect the areas of interest from the T-34A N141SW accident aircraft. Due to the recent history of fatigue cracking and failure, a destructive evaluation of the T-34A would be useful to the FAA for specifically addressing T-34A concerns and, in a general sense, assessing the condition of a high-time acrobatic category aircraft. The following four areas of interest from the N141SW accident aircraft were examined for cracks and corrosion:

- Right wing front carry-through lower spar
- Horizontal and vertical stabilizer attachment points
- Right wing rear spar lower cap at WS 66
- Right wing rear spar lower bathtub fitting

Cracks found on these areas of the accident aircraft were opened, and the crack faces were analyzed to determine failure mode. The surrounding structure was also inspected microscopically for additional defects. A typical T-34A aircraft is pictured in figure 1.



FIGURE 1. TYPICAL T-34A AIRCRAFT

## 2. TEARDOWN EVALUATION.

The wreckage from the December 7, 2004, accident involving a Beechcraft T-34A, tail number N141SW, was disassembled and microscopically examined to determine if pre-existing fatigue cracks were prevalent in four areas of interest on the aircraft. These areas were extracted from the surrounding structure and fully disassembled to enable an examination of crack face characteristics. Several areas also had various nondestructive inspections performed. Total crack lengths and failure modes are shown in the subsequent figures. Cracks were given numbers for identification purposes as shown in the figures.

Figure 2 shows the wreckage as it was received prior to disassembly. All sections of the aircraft were received, except for several areas on the left wing that were previously removed by the NTSB for examination.

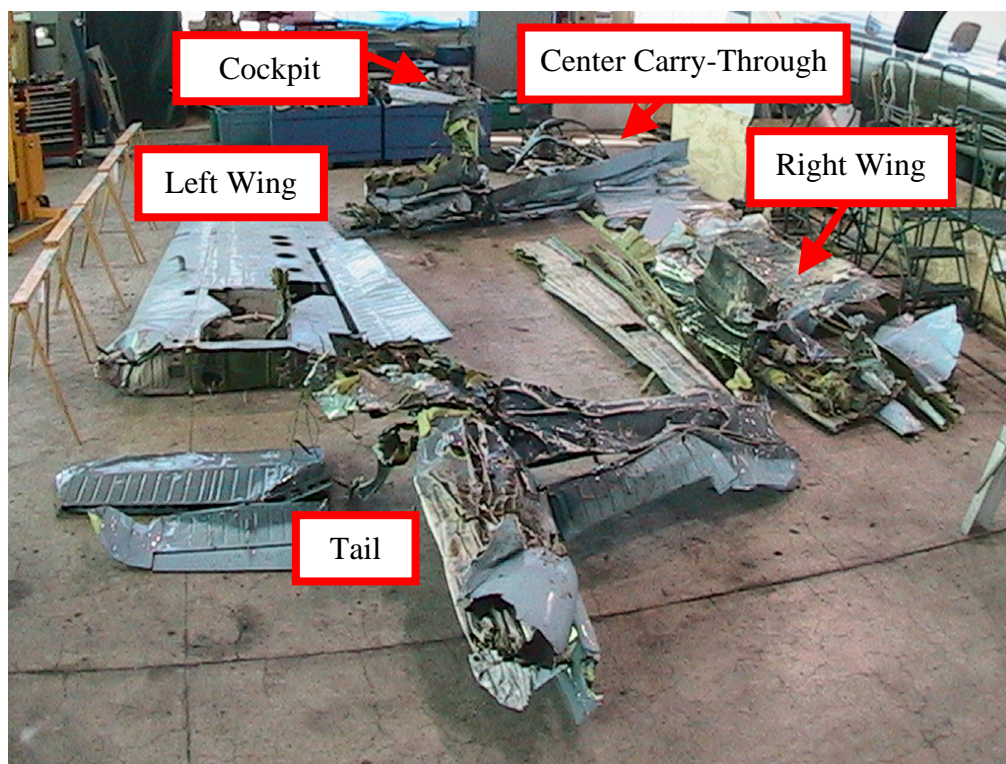


FIGURE 2. WRECKAGE AS RECEIVED

The following four areas were determined by the FAA to be areas of interest and were examined for fatigue cracks:

- Right wing front carry-through lower spar
- Horizontal and vertical stabilizer attachment points
- Right wing rear spar lower cap WS 66
- Right wing rear spar lower bathtub fitting

## 2.1 SURFACE EDDY-CURRENT NONDESTRUCTIVE INSPECTION.

The right wing front carry-through was partially disassembled, and a surface scan eddy-current inspection was performed around nine attachment boltholes on both the forward and aft sides of the structure. This scan indicated a crack on the aft side of the right wing front carry-through outer (-33) channel, shown in figure 3. Other cracks on this same detail were not detected using surface scan eddy current due to excessive crushing of the structure during impact, which limited inspection access.

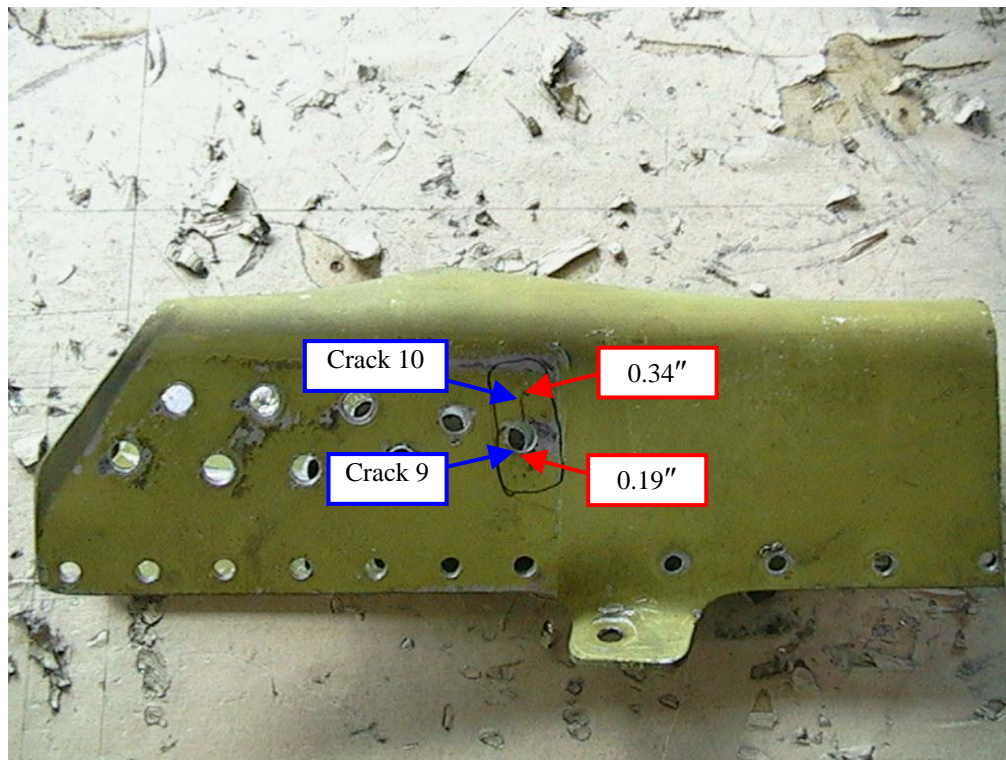


FIGURE 3. AFT SIDE OF THE RIGHT WING FRONT CARRY-THROUGH OUTER (-33) CHANNEL, CRACKS 9 AND 10

## 2.2 DISASSEMBLY PHASE.

Only the areas of interest were disassembled, while all other structure was returned to the NTSB. Figures 4 through 7 show the as-received condition of the four areas that were disassembled and examined.



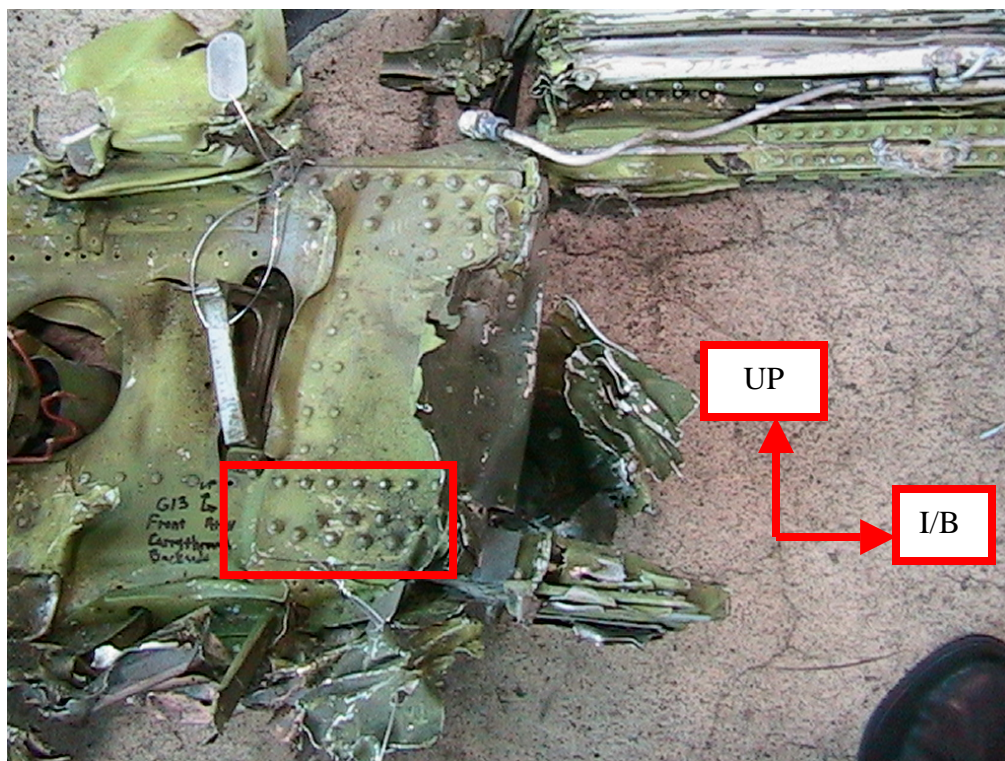


FIGURE 4. RIGHT WING FRONT CARRY-THROUGH LOWER SPAR

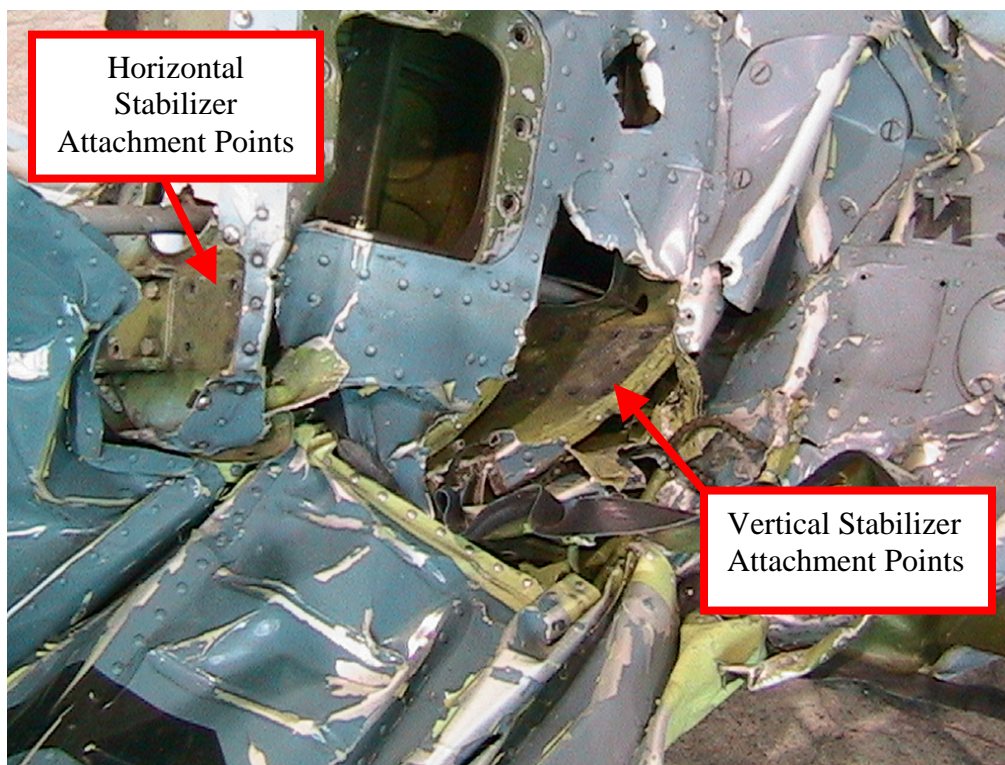


FIGURE 5. HORIZONTAL AND VERTICAL STABILIZER ATTACHMENT POINTS





FIGURE 6. RIGHT WING REAR SPAR WS 66



FIGURE 7. RIGHT WING REAR SPAR LOWER BATHTUB FITTING

## 2.3 MICROSCOPIC EXAMINATION.

A microscopic examination was conducted on the four areas of interest. The inspection procedure consisted of examining all components of the areas of interest under a 7-45 power microscope, opening and examining fracture faces under low magnification, and if necessary viewing fracture faces under a scanning electron microscope (SEM) to assist in determining failure mode.

Cracks with the following identification numbers were opened and subjected to a microscopic examination in order to determine failure mode: Cracks 1-5, 7, 8, 10, 12-14, 16-38. Cracks 6, 9, 11, and 15 were not opened for examination due either to their proximity and similarity to other cracks that were examined as part of this effort or to their location on the part prohibiting examination of the fracture surface.

### 2.3.1 Right Wing Front Carry-Through.

Twenty-five cracks were found on the right wing front carry-through, which is composed of three channels and web skins, as shown in figure 8.

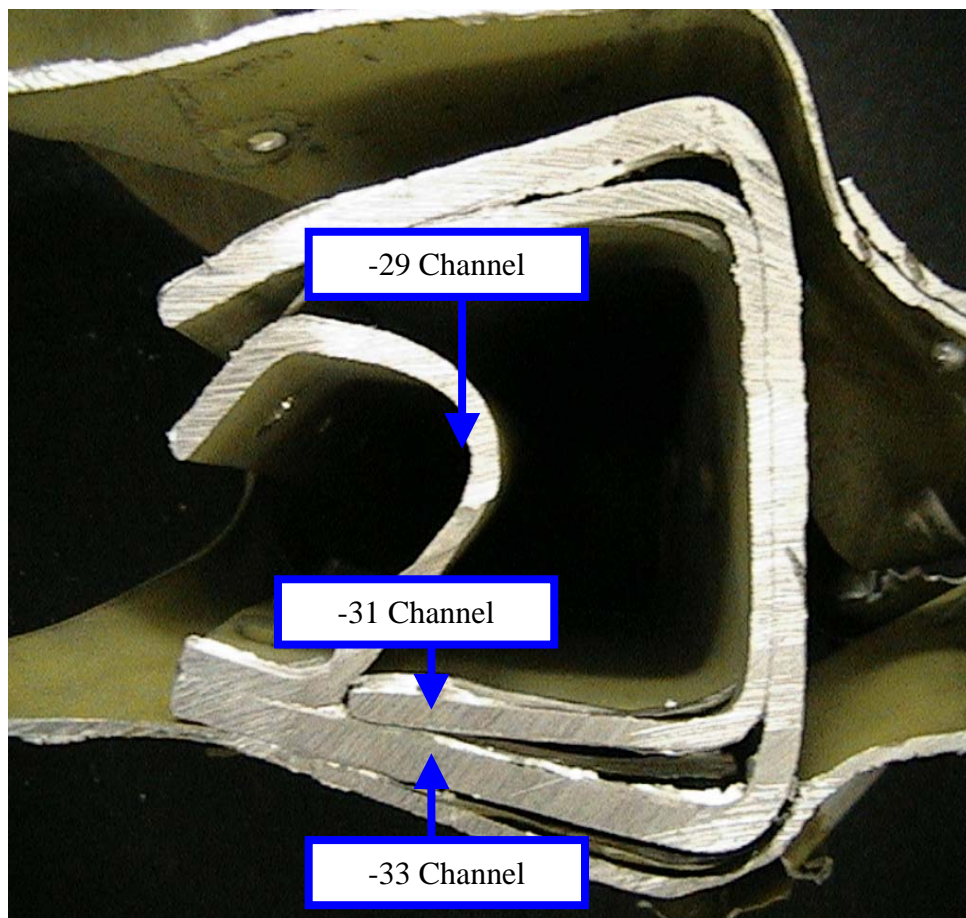


FIGURE 8. RIGHT WING FRONT CARRY-THROUGH STACKUP



### 2.3.1.1 Right Wing Front Carry-Through Middle (-31) Channel.

The right wing front carry-through was examined microscopically for cracks and corrosion. Figure 9 shows the locations of two cracks, cracks 1 and 2, on the right wing front carry-through middle channel forward side, part number 45-410215-31. Most cracks found on the right wing front carry-through began as fatigue cracks, but were lengthened due to overload. Crack 1 had a total length of 0.63 inch. The initial 0.14 inch of this crack failed due to fatigue, with the remaining growth due to overload. The crack face, shown in figure 10, shows that the origin of the crack was located near the edge of a fastener hole. Crack 2 was 0.73 inch long, and its fracture face is shown in figure 11. As shown in this figure, the initial 0.08 inch of growth was due to fatigue, with the next 0.19 inch of growth due to unstable fatigue. All subsequent growth occurred due to overload.

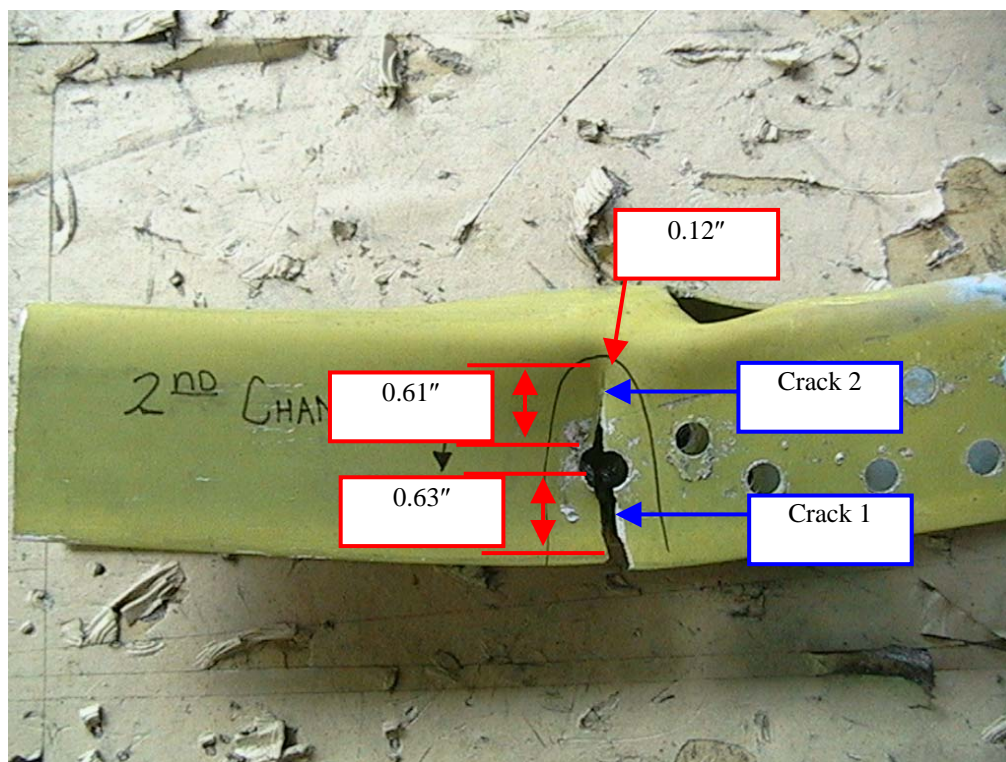


FIGURE 9. LOCATIONS OF CRACKS 1 AND 2 ON THE RIGHT WING FRONT CARRY-THROUGH MIDDLE (-31) CHANNEL FORWARD SIDE

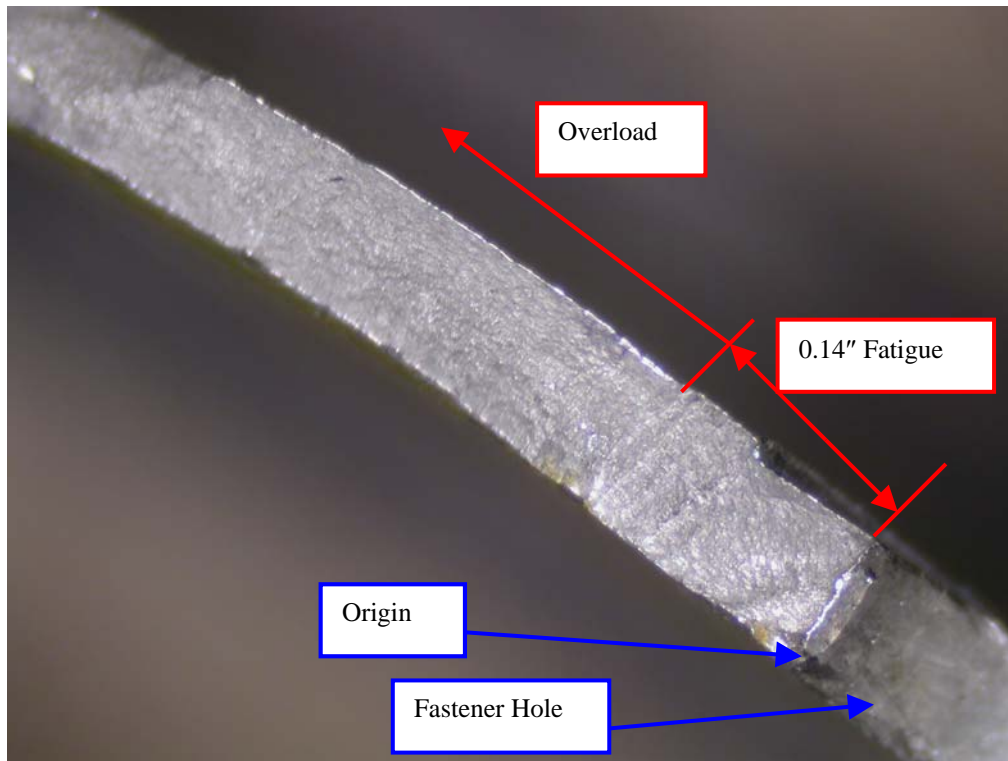


FIGURE 10. CRACK 1 FRACTURE FACE

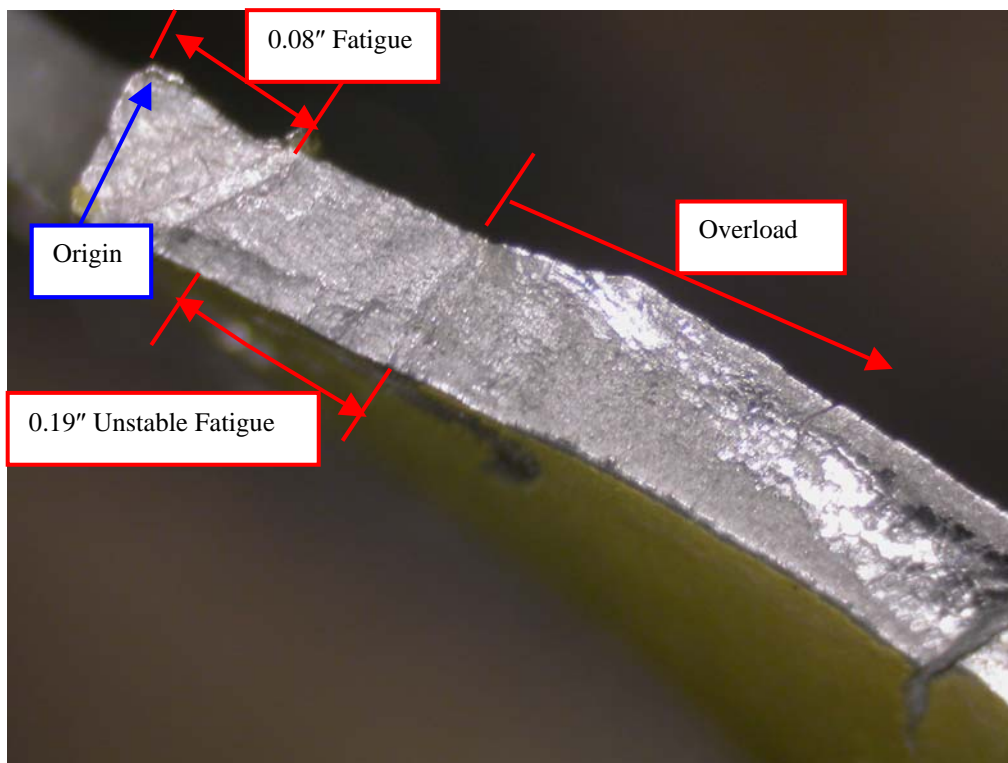


FIGURE 11. CRACK 2 FRACTURE FACE



Figure 12 shows the locations of cracks 3 and 4 on the right wing front carry-through middle channel aft side, part number 45-410215-31. The fracture face for crack 3 is shown in figure 13, showing the location of the origin. The initial 0.32 inch of crack growth was caused by fatigue with the remaining 0.28 inch caused by overload. The fracture face of crack 4, shown in figure 14, provides the location of the origin for this 0.79-inch crack. It also shows the fatigue region of growth, which measures 0.42 inch, with the remaining growth of the crack due to overload.

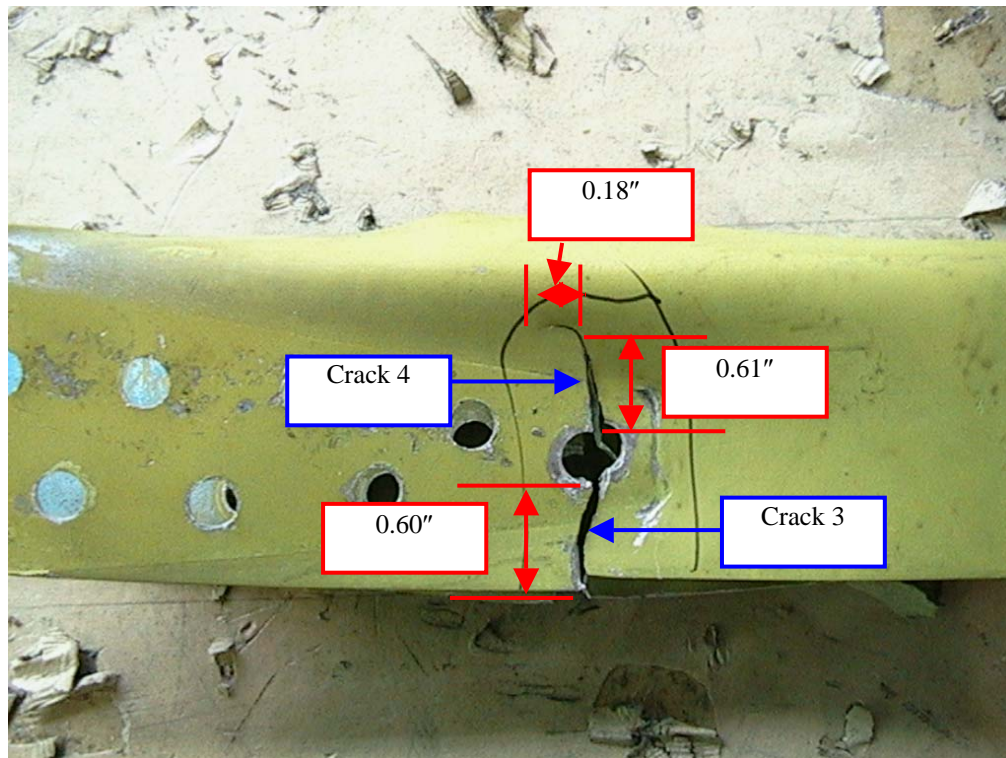


FIGURE 12. LOCATIONS OF CRACKS 3 AND 4 ON THE RIGHT WING FRONT CARRY-THROUGH MIDDLE (-31) CHANNEL AFT SIDE

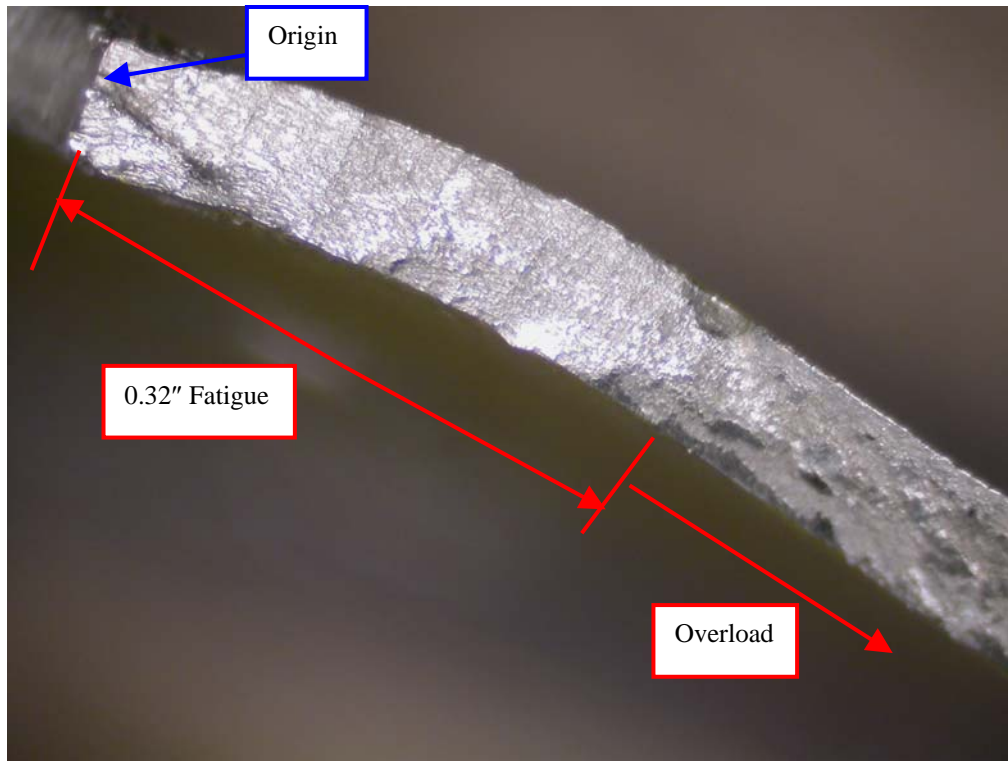


FIGURE 13. CRACK 3 FRACTURE FACE

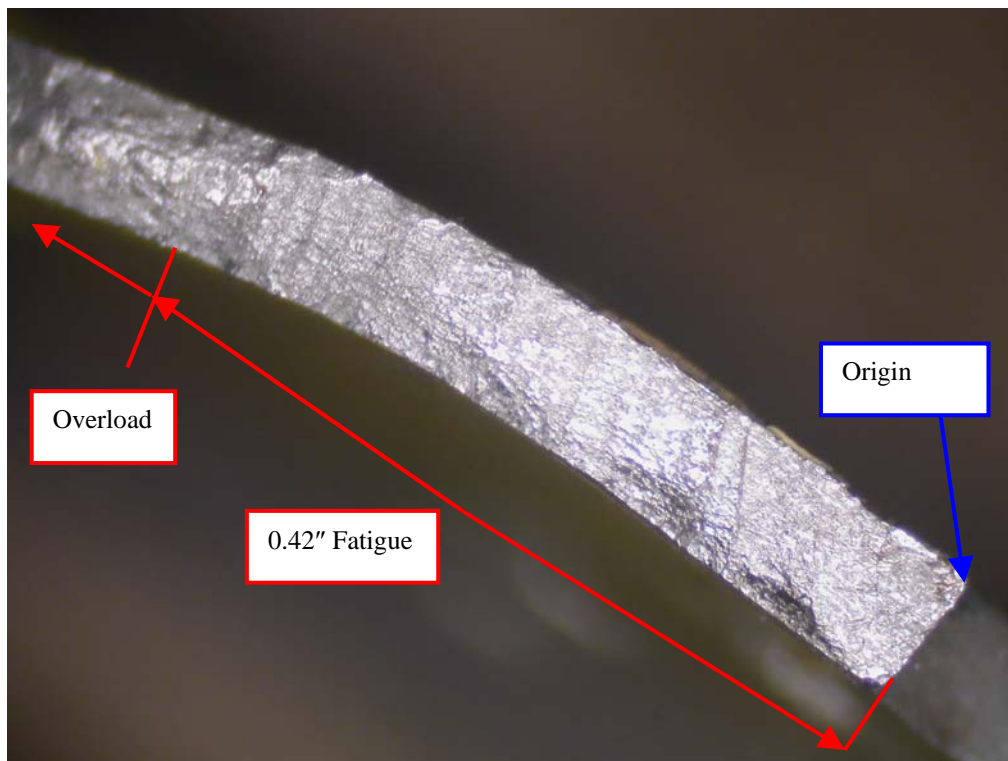


FIGURE 14. CRACK 4 FRACTURE FACE

The locations of two cracks, identified as cracks 5 and 6, on the right wing front carry-through middle channel lower surface, part number 45-410215-31, are shown in figure 15. A picture of the crack 5 fracture face is provided in figure 16. This figure shows the location of the origin of this 0.09-inch-long crack. The shape of the 0.08-inch-long fatigue region is also shown in figure 16, illustrating that crack 5 had not grown completely through the thickness of the channel. Crack 6, which had a total length of 0.13 inch, was not opened for examination.

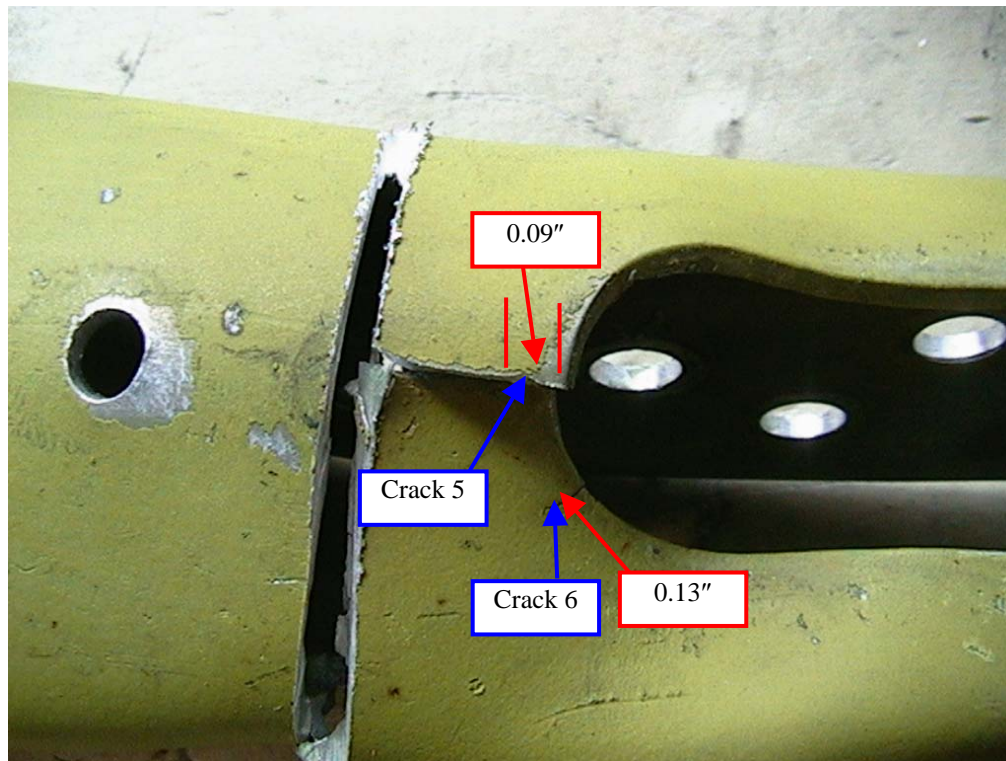


FIGURE 15. LOCATIONS OF CRACKS 5 AND 6 ON THE RIGHT WING FRONT CARRY-THROUGH MIDDLE (-31) CHANNEL LOWER SURFACE

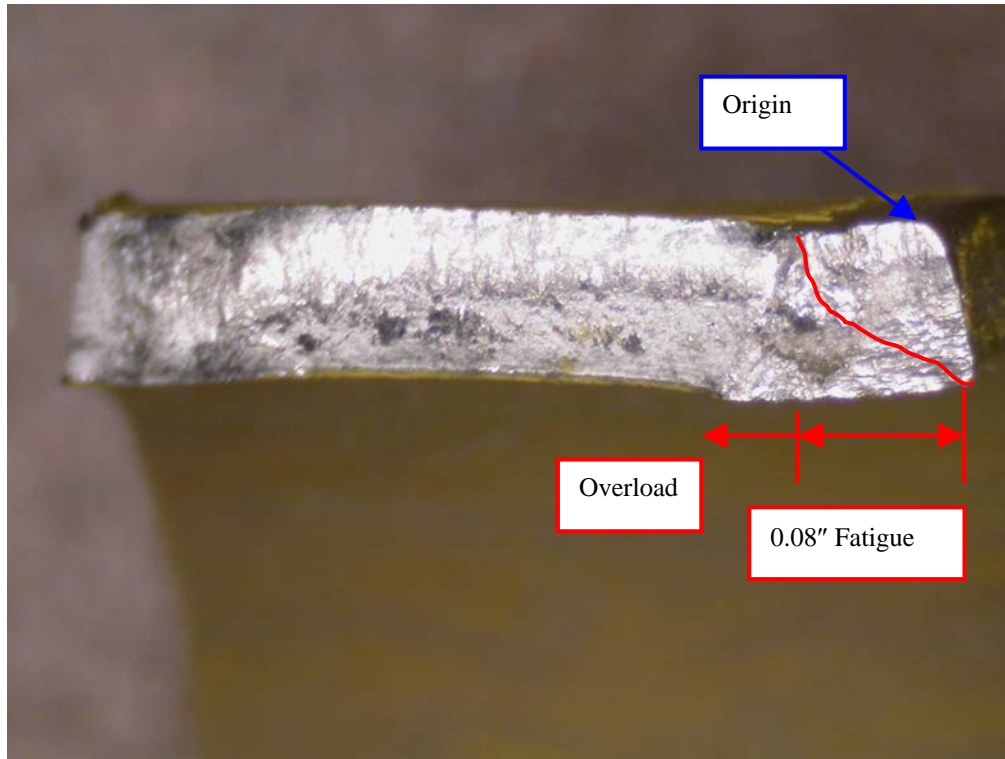


FIGURE 16. CRACK 5 FRACTURE FACE

#### 2.3.1.2 Right Wing Front Carry-Through Outer (-33) Channel.

Figure 17 shows the locations of cracks 7 and 8 on the right wing front carry-through outer channel forward side, part number 45-410215-33. Crack 7 measured 0.15 inch in length and was caused solely by overload. The fracture face of crack 8, which measured 0.17 inch in length, is shown in figure 18, showing a 0.15-inch region of fatigue prior to the growth mechanism transitioning to overload. A fractograph of the crack 8 fracture face is shown in figure 19, illustrating the direction of crack growth as well as identifying a few of the more prominent fatigue striations, or crack face features.



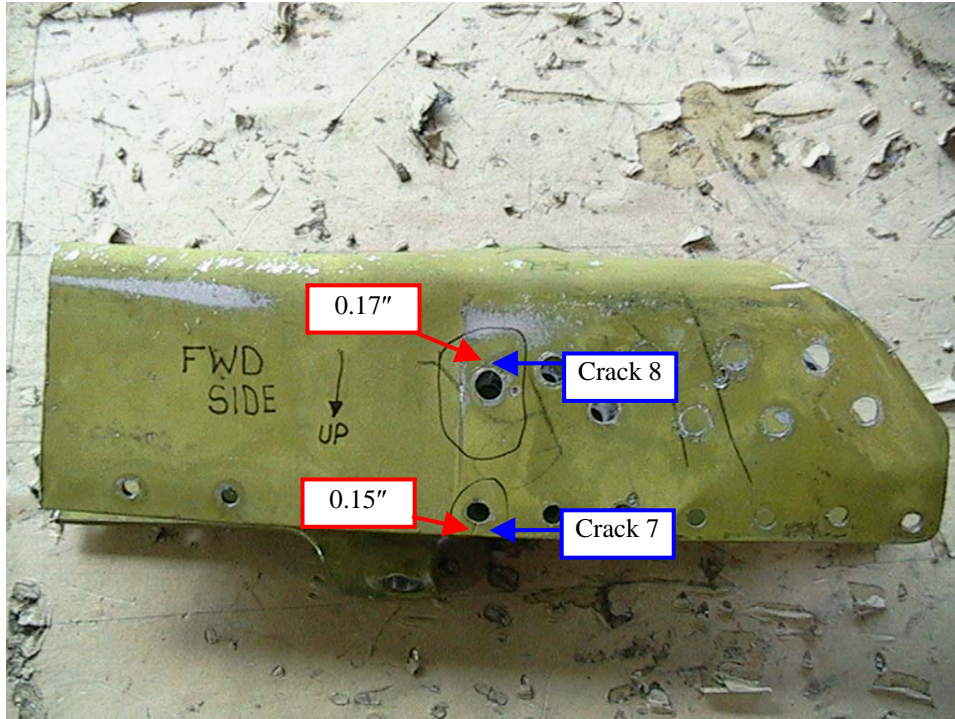


FIGURE 17. LOCATIONS OF CRACKS 7 AND 8 ON THE RIGHT WING FRONT CARRY-THROUGH OUTER (-33) CHANNEL FORWARD SIDE

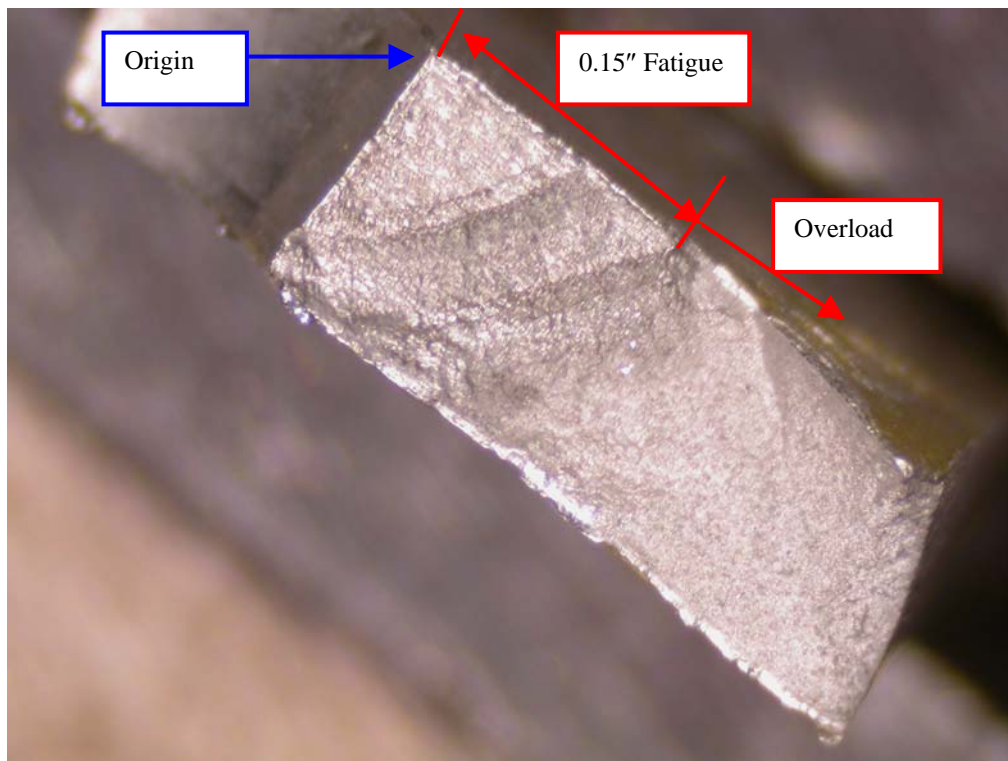


FIGURE 18. CRACK 8 FRACTURE FACE

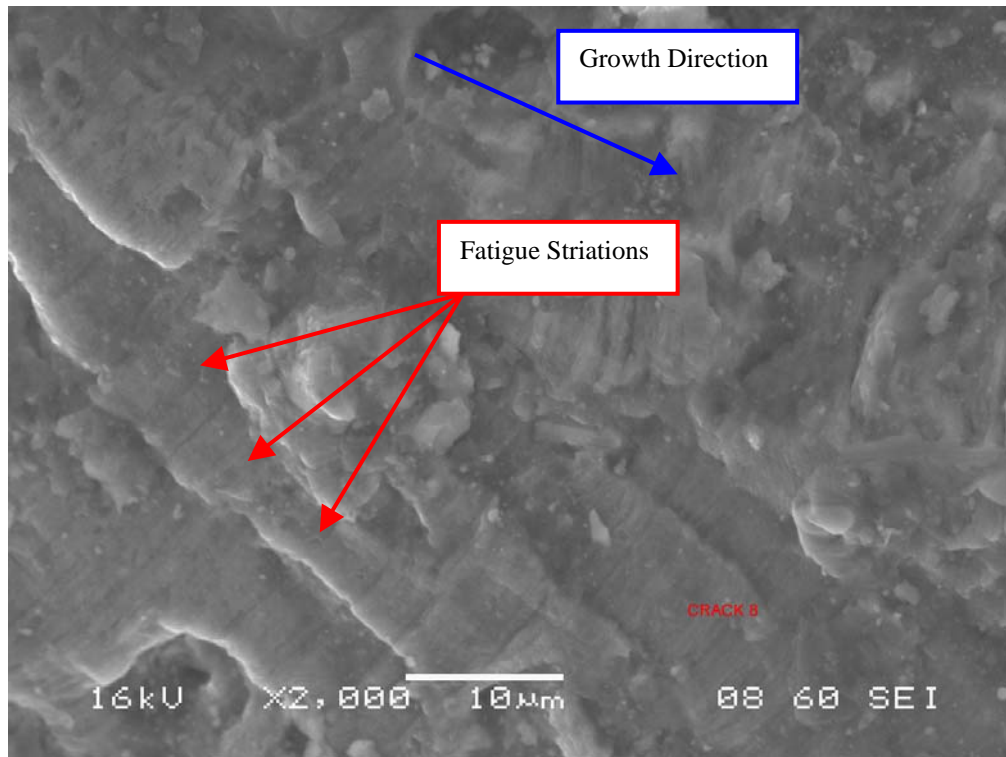


FIGURE 19. SURFACE FACE SEM FRACTOGRAPH OF CRACK 8

Figure 20 shows the locations of cracks 9 and 10 on the right wing front carry-through outer (-33) channel aft side. Crack 9 measured 0.19 inch and was not opened for examination. Crack 10 had a total length of 0.34 inch and a fatigue length of 0.27 inch, as shown in figure 21. This picture of the crack face also shows the location of the origin and the region of failure due to overload. Crack 10 had not propagated through the entire thickness of the channel. Figure 22 shows a fractograph of crack 10 with the growth direction indicated and prominent fatigue striations identified.

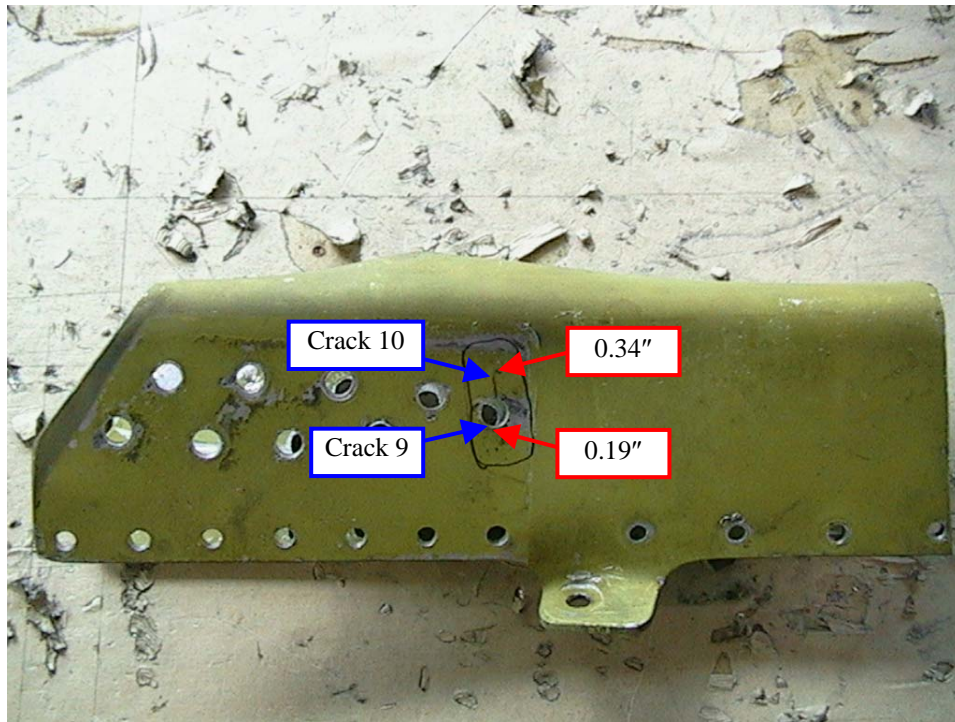


FIGURE 20. LOCATIONS OF CRACKS 9 AND 10 ON THE RIGHT WING FRONT CARRY-THROUGH OUTER (-33) CHANNEL AFT SIDE

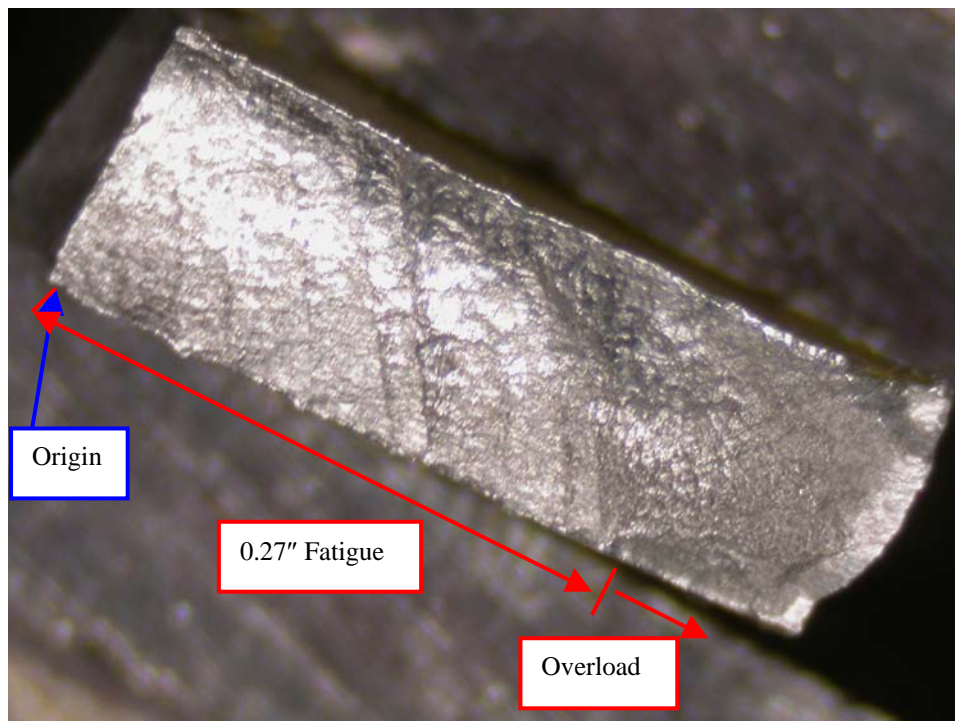


FIGURE 21. CRACK 10 FRACTURE FACE



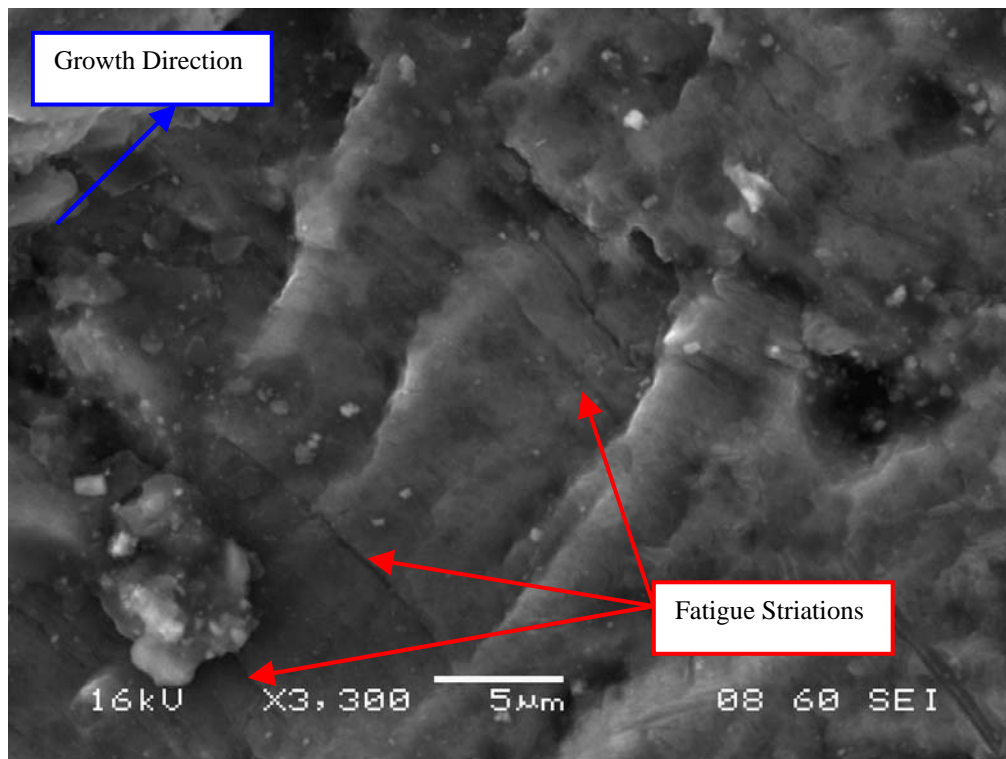


FIGURE 22. SURFACE FACE SEM FRACTOGRAPH OF CRACK 10

Figure 23 shows the locations of cracks 11 and 12 on the right wing front carry-through outer (-33) channel lower surface. Crack 11, which measured 0.10 inch in length, was not opened for examination. Crack 12 had a total length of 0.80 inch with a fatigue region of 0.13 inch, as shown in figure 24. The remaining growth of the crack was due to overload. Fractographs of crack 12 are provided in figures 25 and 26, showing crack propagation directions as well as identifying fatigue striations.



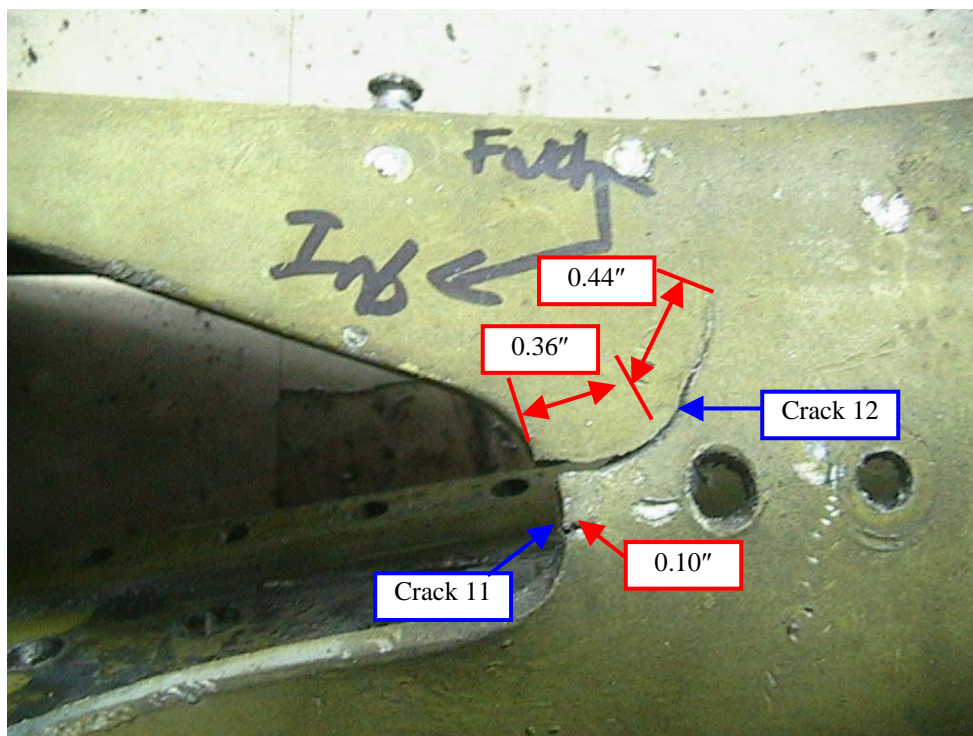


FIGURE 23. LOCATIONS OF CRACKS 11 AND 12 ON THE RIGHT WING FRONT CARRY-THROUGH OUTER (-33) CHANNEL LOWER SURFACE

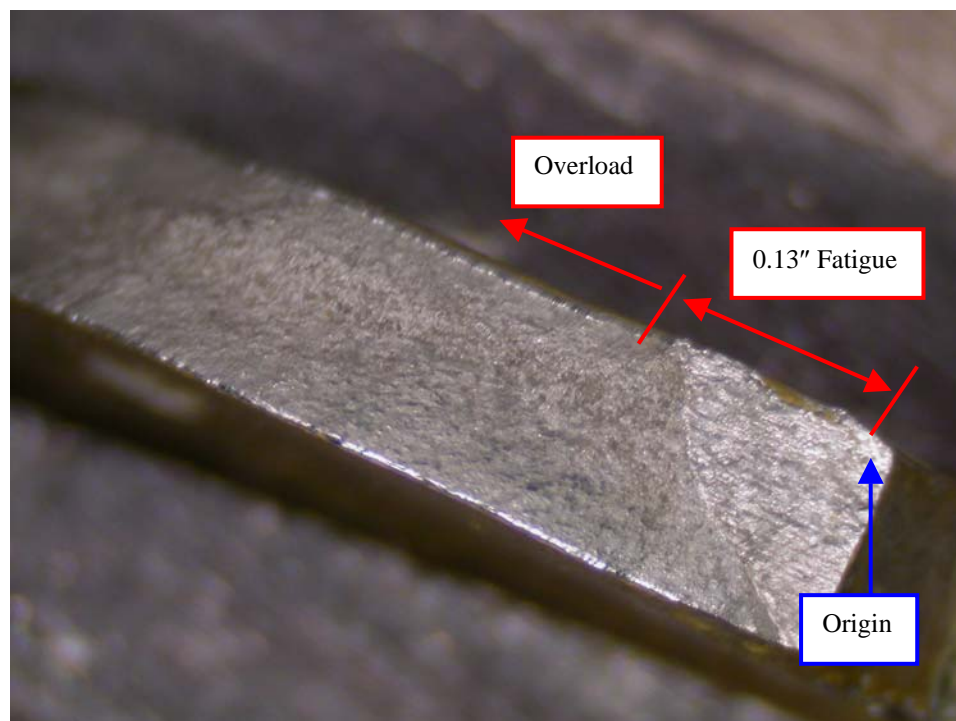


FIGURE 24. CRACK 12 FRACTURE FACE

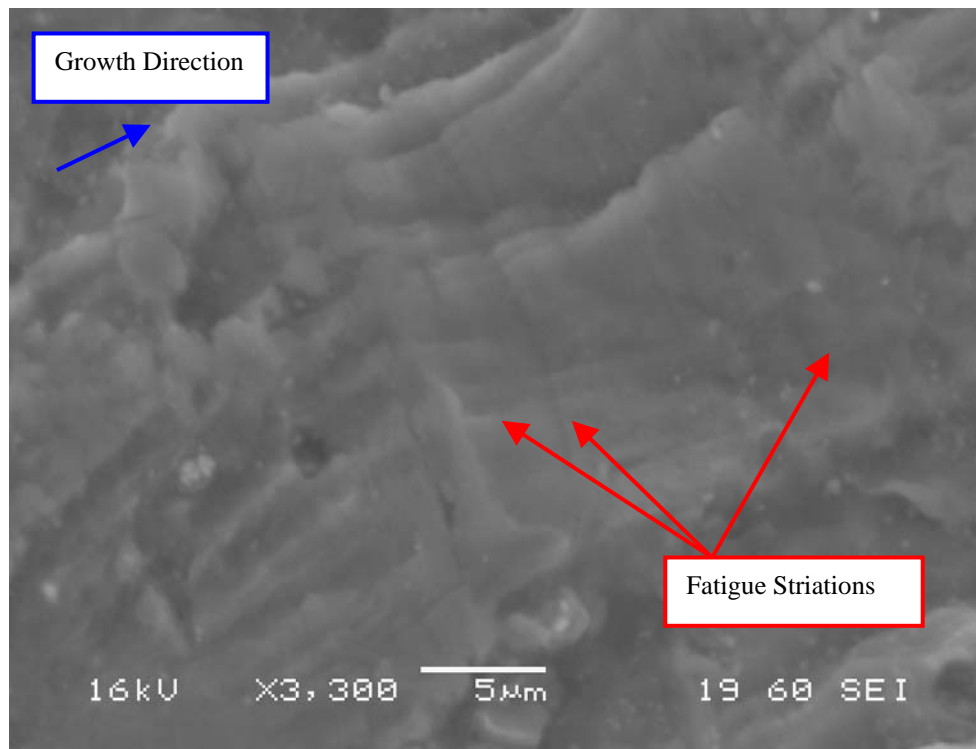


FIGURE 25. SURFACE FACE SEM FRACTOGRAPH OF CRACK 12 (X3,300)

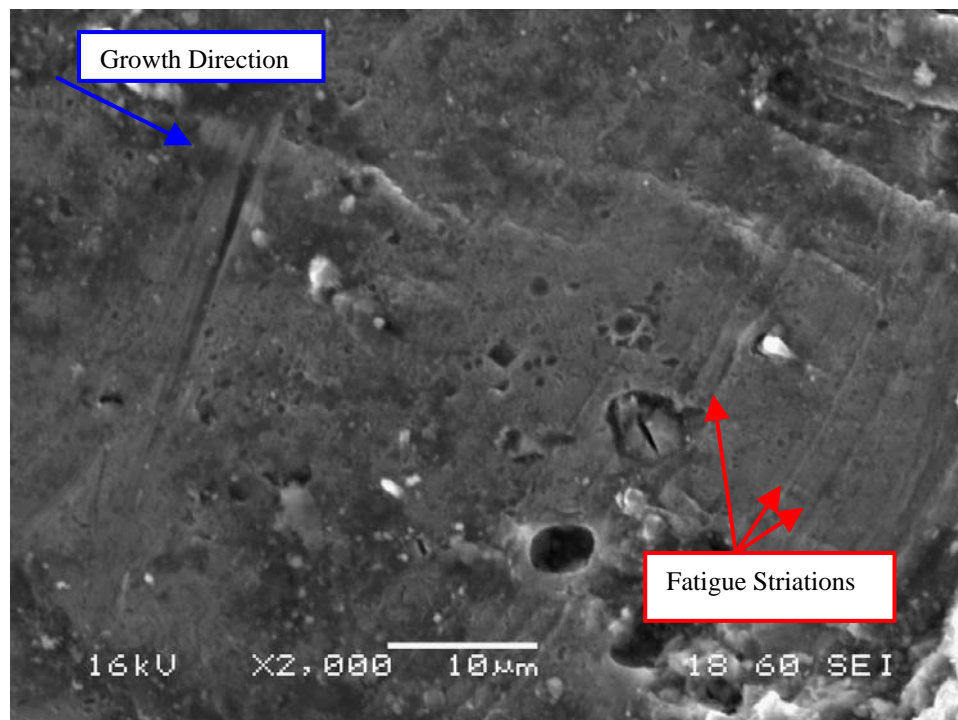


FIGURE 26. SURFACE FACE SEM FRACTOGRAPH OF CRACK 12 (X2,000)

### 2.3.1.3 Right Wing Front Carry-Through Web Skin.

Figure 27 shows the right wing front carry-through aft side structural stackup. The locations of cracks 13-15 are shown in figure 28. Crack 13 had a total length of 0.31 inch with an initial fatigue length of 0.05 inch, which was through the thickness, as shown in figure 29. Figure 29 also shows the location of the origin of this crack. Crack 14 had a total length of 0.52 inch, with an initial fatigue length of 0.22 inch. This crack was also completely through the thickness. The fracture face for crack 14 is provided in figure 30 and shows the location of the origin along with the existence of a transition period of rapid growth, which was comprised of unstable fatigue that extended the crack length 0.05 to 0.10 inch prior to the final growth increment due to overload. Crack 15 had a total length of 0.26 inch and was not opened for examination.

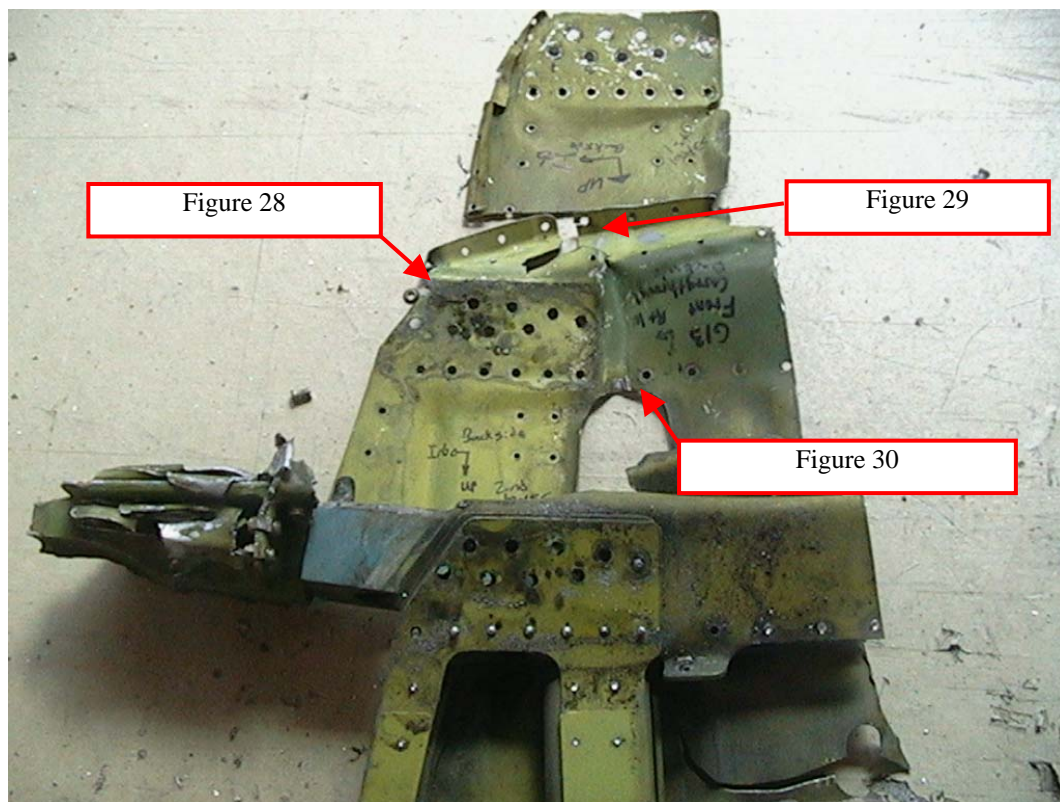


FIGURE 27. RIGHT WING FRONT CARRY-THROUGH AFT SIDE STACKUP



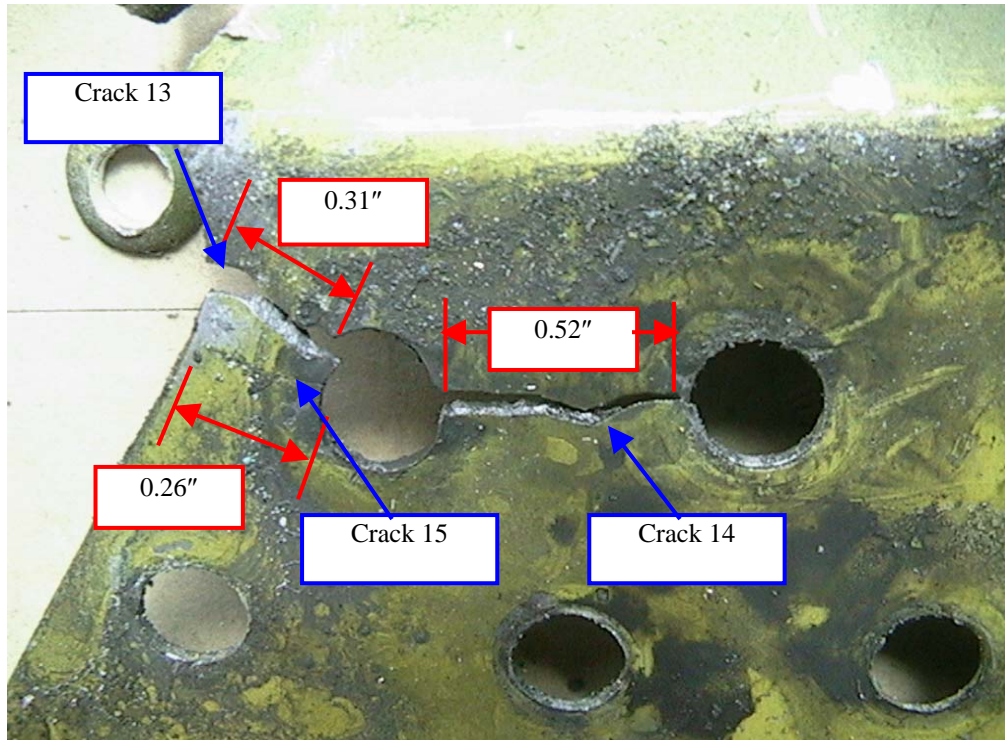


FIGURE 28. LOCATIONS OF CRACKS 13, 14, AND 15 ON THE RIGHT WING FRONT CARRY-THROUGH MIDDLE LAYER AFT SIDE WEB SKIN

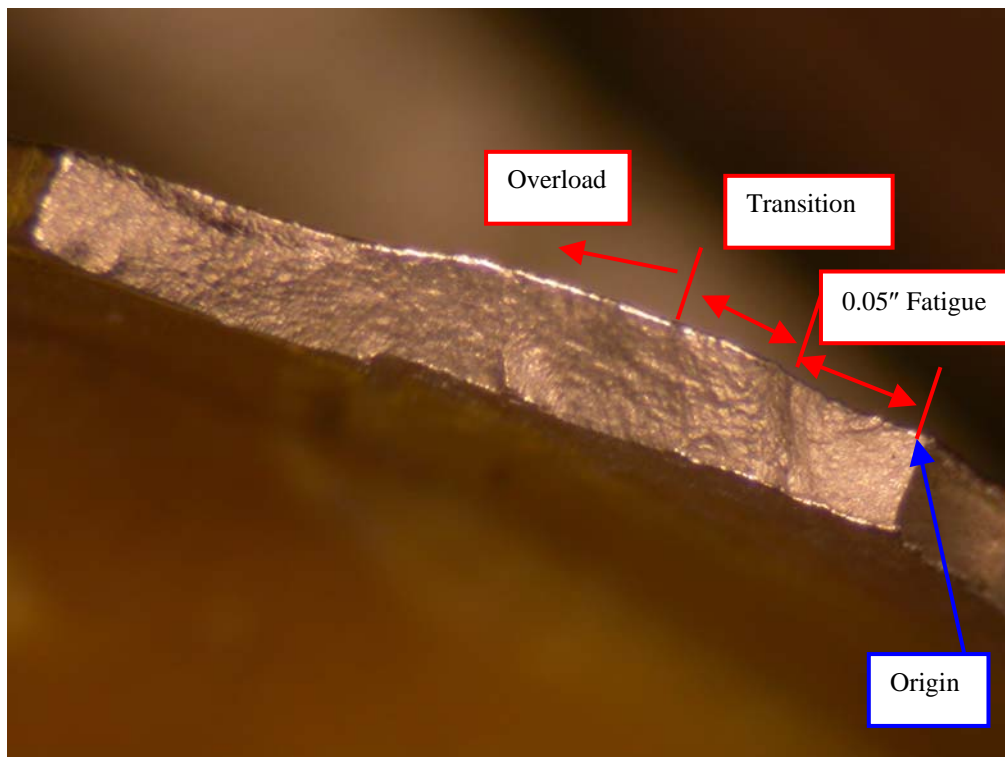


FIGURE 29. CRACK 13 FRACTURE FACE

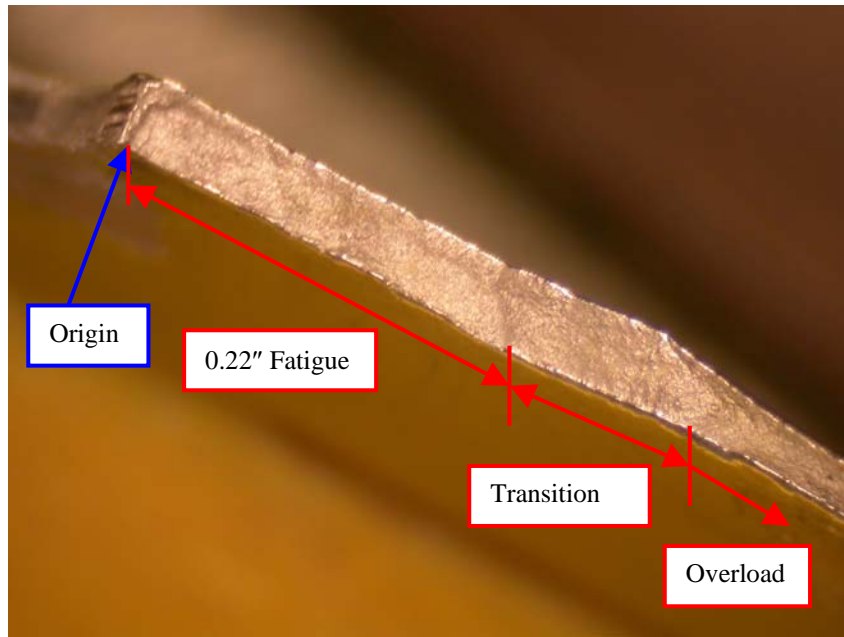


FIGURE 30. CRACK 14 FRACTURE FACE

The locations of cracks 16 and 17 are shown in figure 31. The total length of crack 16 was 1.12 inches, while the total length of crack 17 was 1.17 inches. Both of these cracks were opened and examined, but due to extensive metal smearing of the crack faces, no failure mode could be determined.

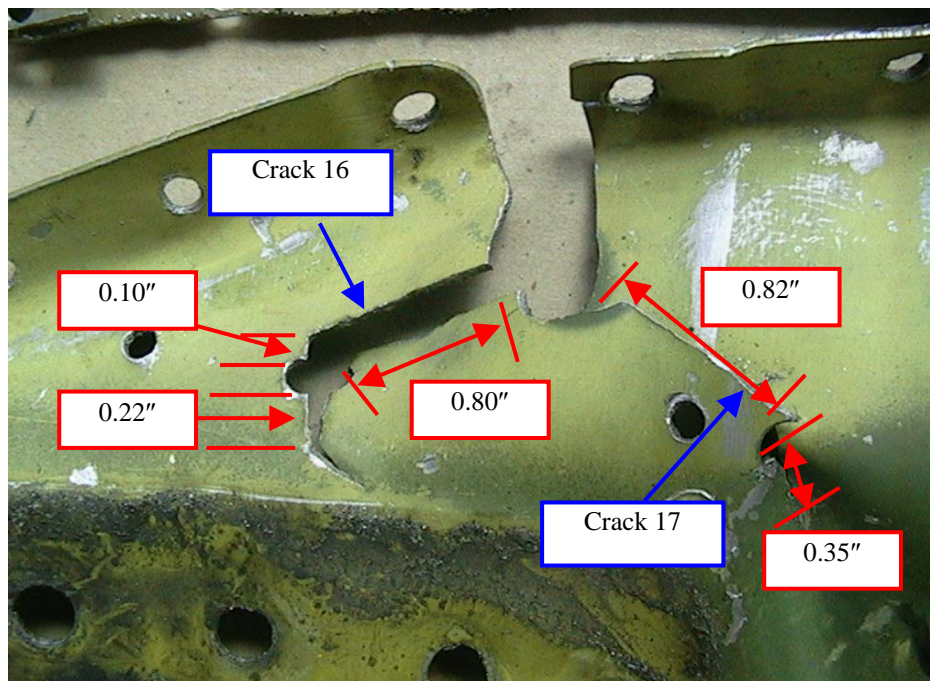


FIGURE 31. LOCATIONS OF CRACKS 16 AND 17 ON THE RIGHT WING FRONT CARRY-THROUGH MIDDLE LAYER AFT SIDE WEB SKIN

Figure 32 shows an overview of the locations of cracks 18-22, while the location of each crack is shown in greater detail in figure 33. Crack 18 had a total length of 0.53 inch, and the entire crack was caused by fatigue. The crack had origination points starting at the aft side of the web skin and did not grow into or out of any fastener holes. The fatigue did extend through the entire thickness at times, but not for the entire length of the crack. The fracture face for crack 18 is shown in figure 34. Crack 19, measuring 0.20 inch in length, was also caused solely by fatigue and originated from the fastener hole on the forward side of the web skin. Figure 35 shows the fracture face for crack 19. The fracture face for crack 20 is shown in figure 36. This figure illustrates the location of the origin of the crack as well as the shape of the crack as it propagated. The entire length of the crack, 0.14 inch, was caused by fatigue. Figure 37 shows the fracture face of crack 21, including the shape of the crack face as it propagated in fatigue a total length of 0.09 inch. Figure 37 also illustrates the location of the origin of crack 21. Crack 22 measured 0.27 inch and failed due solely to overload.

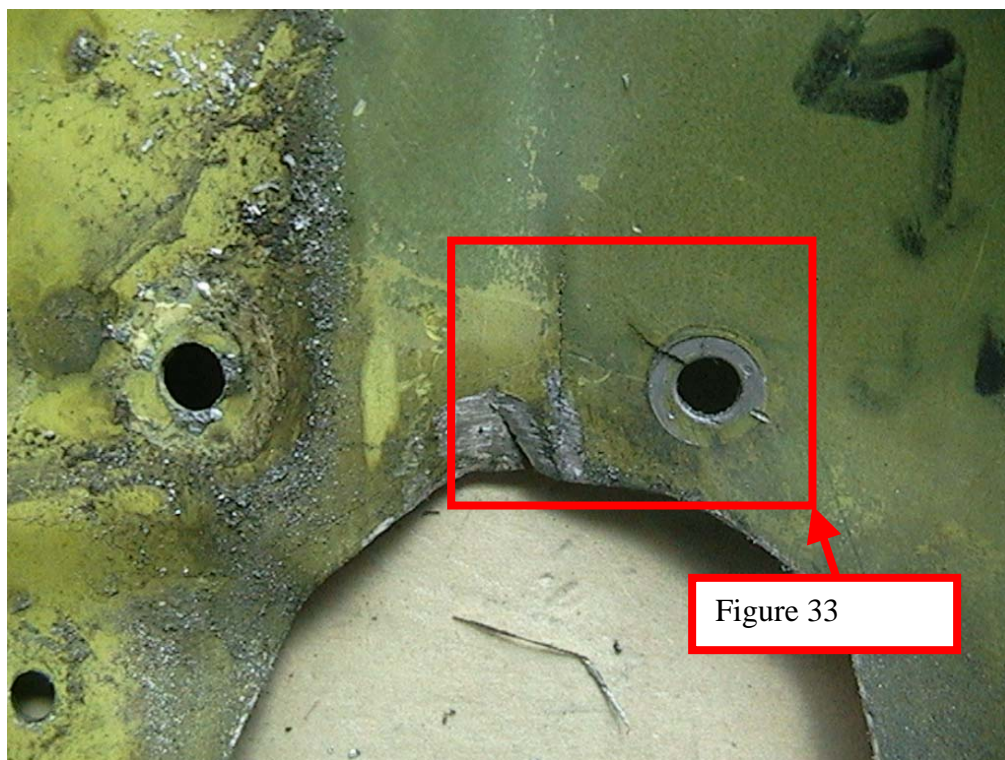


FIGURE 32. LOCATIONS OF CRACKS 18-22 ON THE RIGHT WING FRONT SPAR CARRY-THROUGH MIDDLE LAYER AFT SIDE WEB SKIN



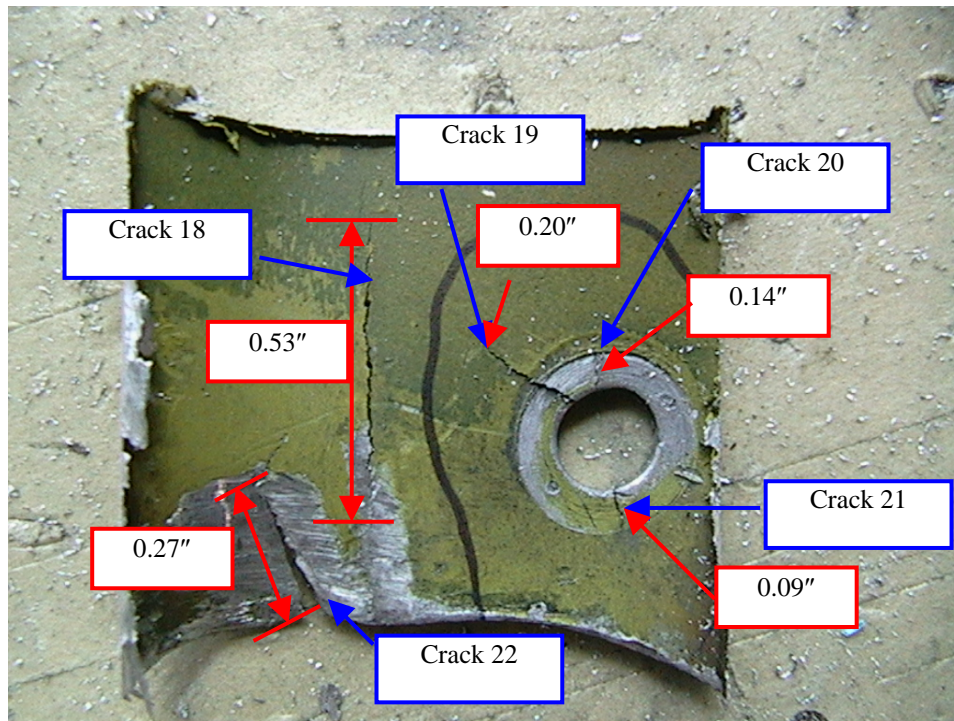


FIGURE 33. DETAILED LOCATIONS OF CRACKS 18-22 ON THE RIGHT WING FRONT SPAR CARRY-THROUGH MIDDLE LAYER AFT SIDE WEB SKIN

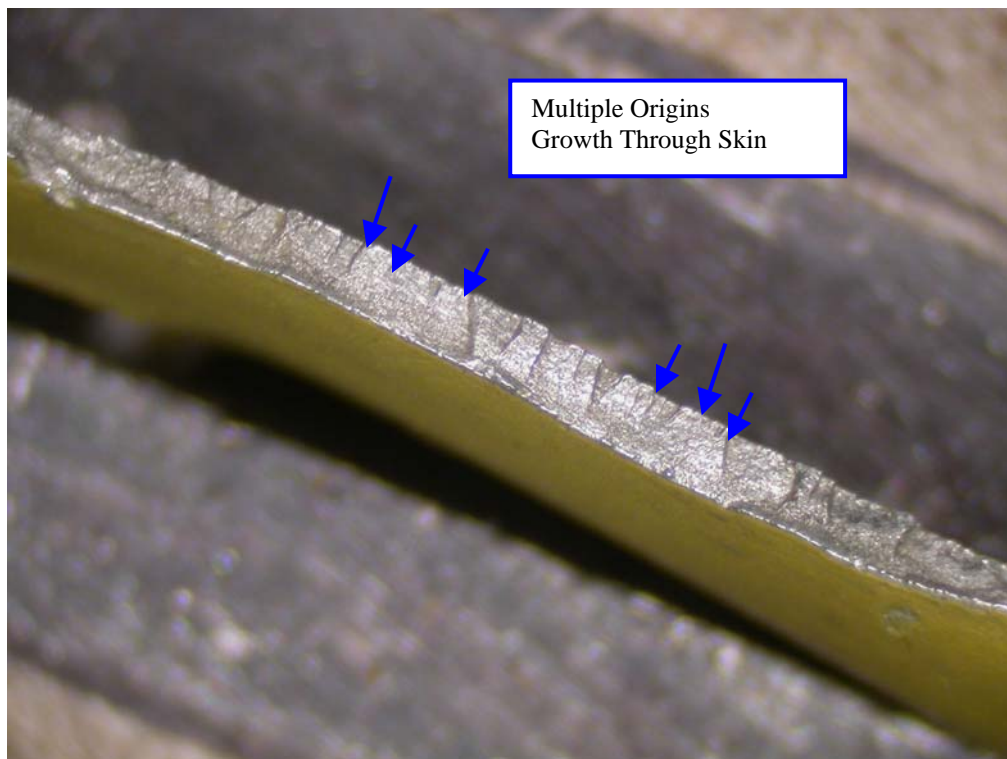


FIGURE 34. CRACK 18 FRACTURE FACE

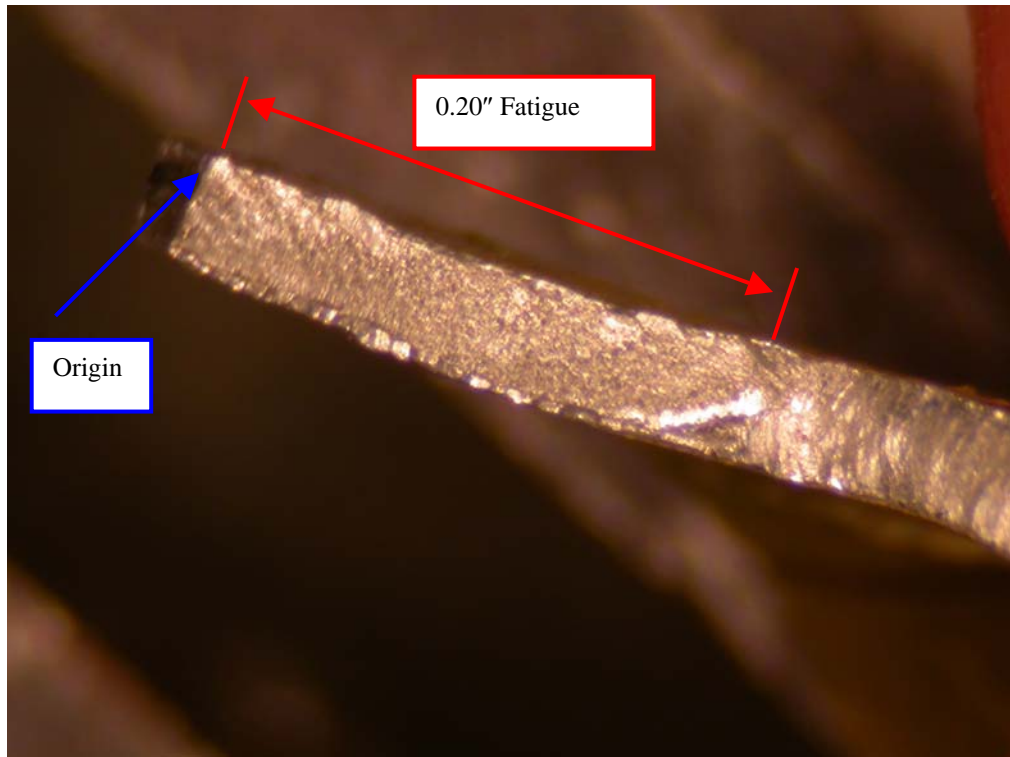


FIGURE 35. CRACK 19 FRACTURE FACE

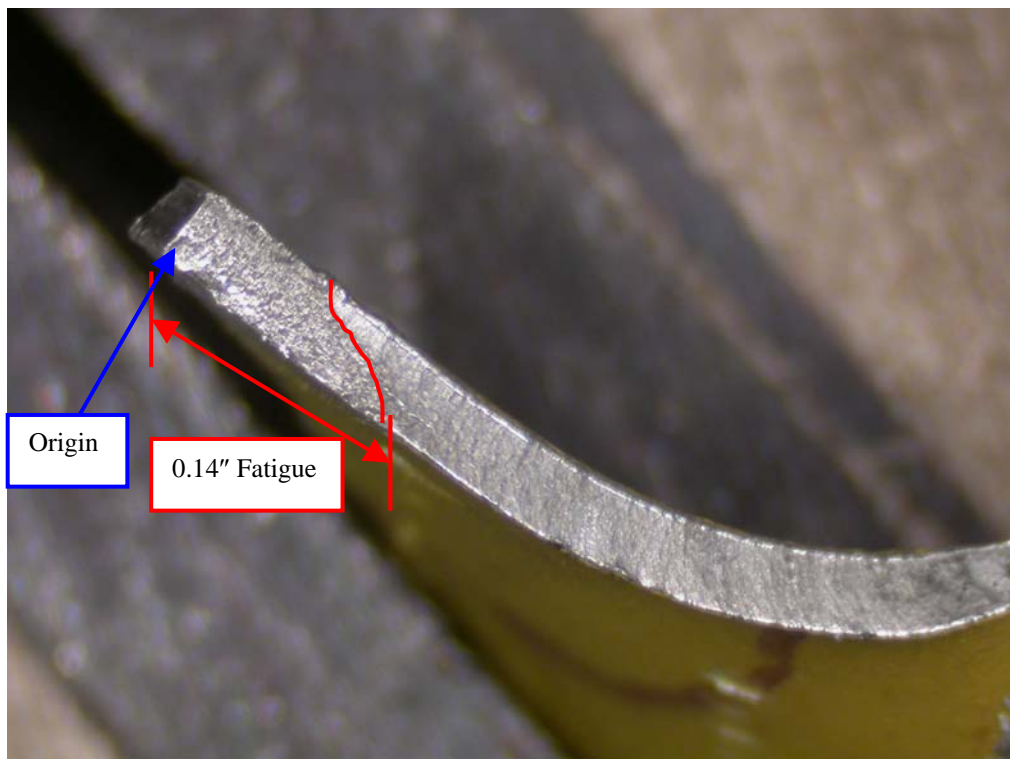


FIGURE 36. CRACK 20 FRACTURE FACE



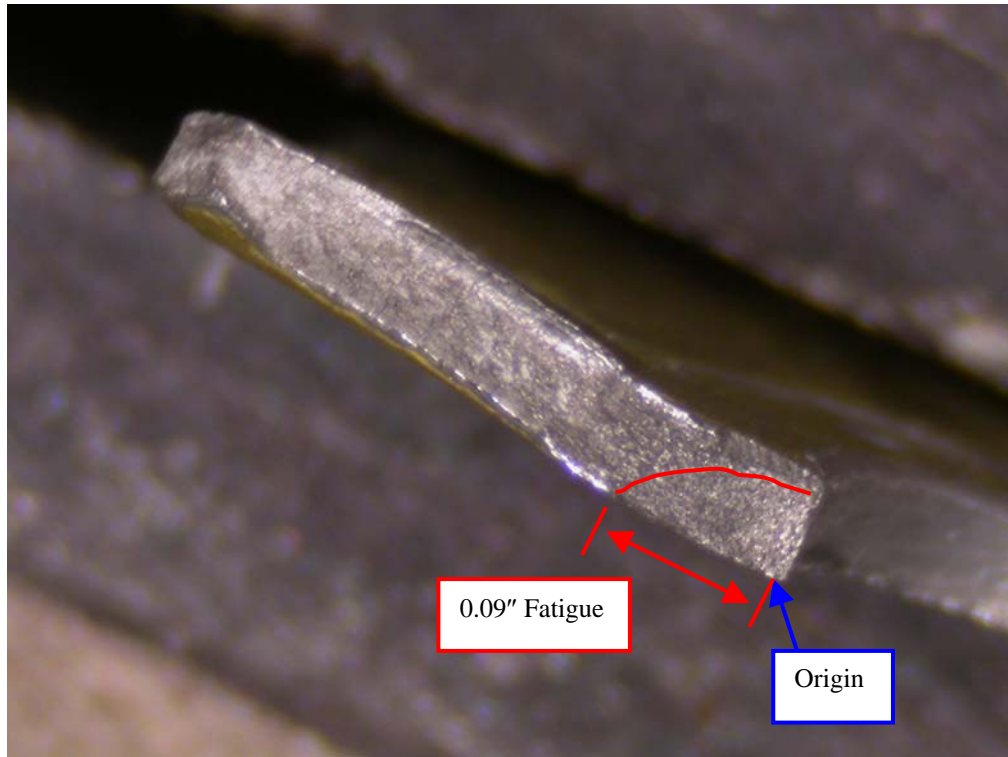


FIGURE 37. CRACK 21 FRACTURE FACE

Figure 38 shows the right wing front carry-through forward side stackup. Figure 39 shows the location of crack 23, which had a total length of 5.28 inches and was caused solely by overload. Figure 40 shows the locations of cracks 24 and 25. Crack 24 had a total length of 0.99 inch with a fatigue length of 0.79 inch. This crack had fatigue origins from the forward side of the web skin. The fracture face for crack 24 is shown in figure 41. Crack 25 had a total length of 0.21 inch, with an initial fatigue length of 0.18 inch. This crack had similar origination points as crack 24, and both cracks were though the thickness at some points but not for the entire length of the crack. The faces of cracks 24 and 25 were severely damaged from rubbing against each other, which makes it difficult to identify individual origins and crack shapes. It is possible that the hole between the cracks is actually a stop-drilled hole, which is an effort to prevent further fatigue crack growth. This idea has not been proven and is only supposition at this point.



FIGURE 38. RIGHT WING FRONT CARRY-THROUGH FORWARD SIDE STACKUP

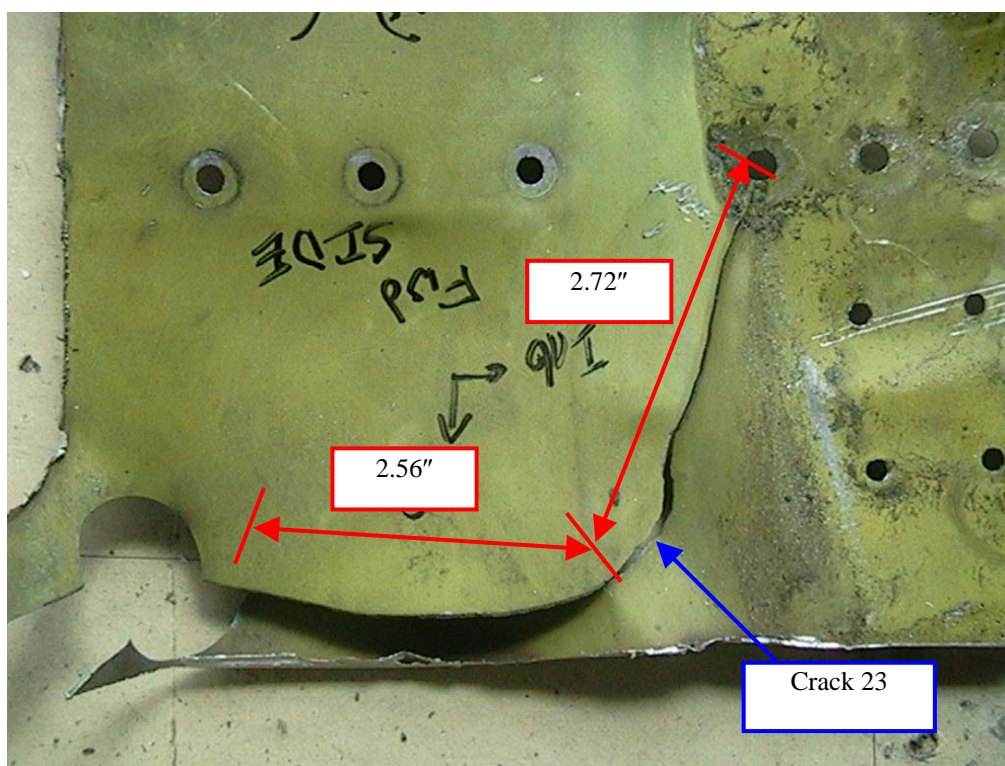


FIGURE 39. LOCATION OF CRACK 23 ON THE RIGHT WING FRONT CARRY-THROUGH MIDDLE LAYER FORWARD SIDE WEB SKIN



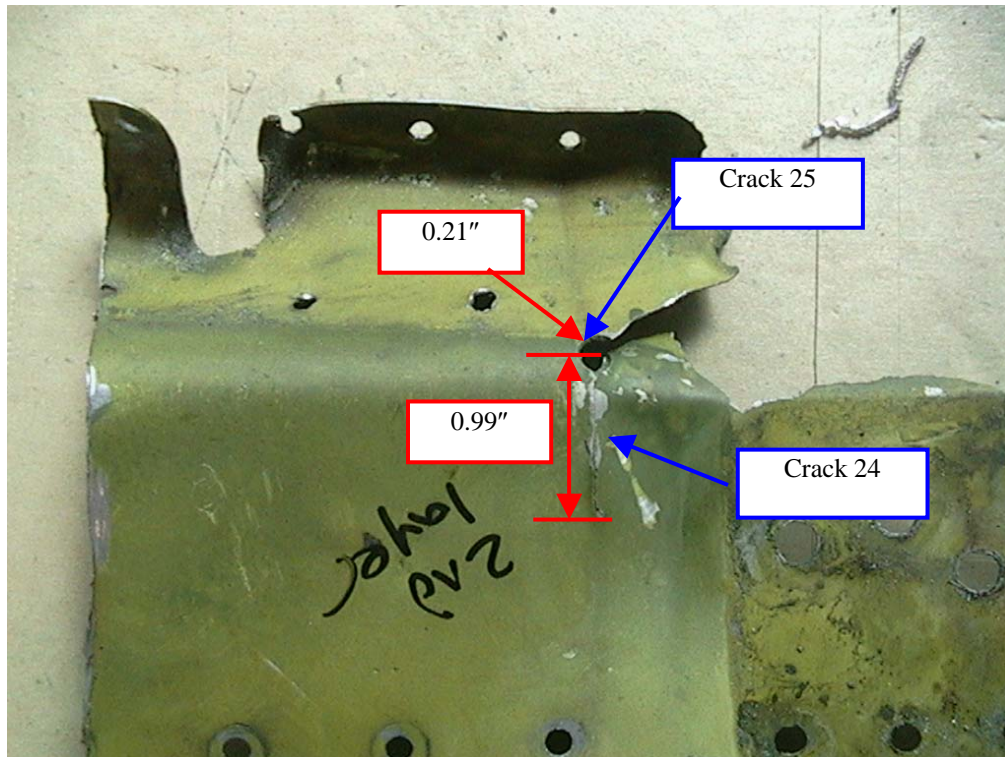


FIGURE 40. LOCATIONS OF CRACKS 24 AND 25 ON THE RIGHT WING FRONT CARRY-THROUGH MIDDLE LAYER FORWARD SIDE WEB SKIN

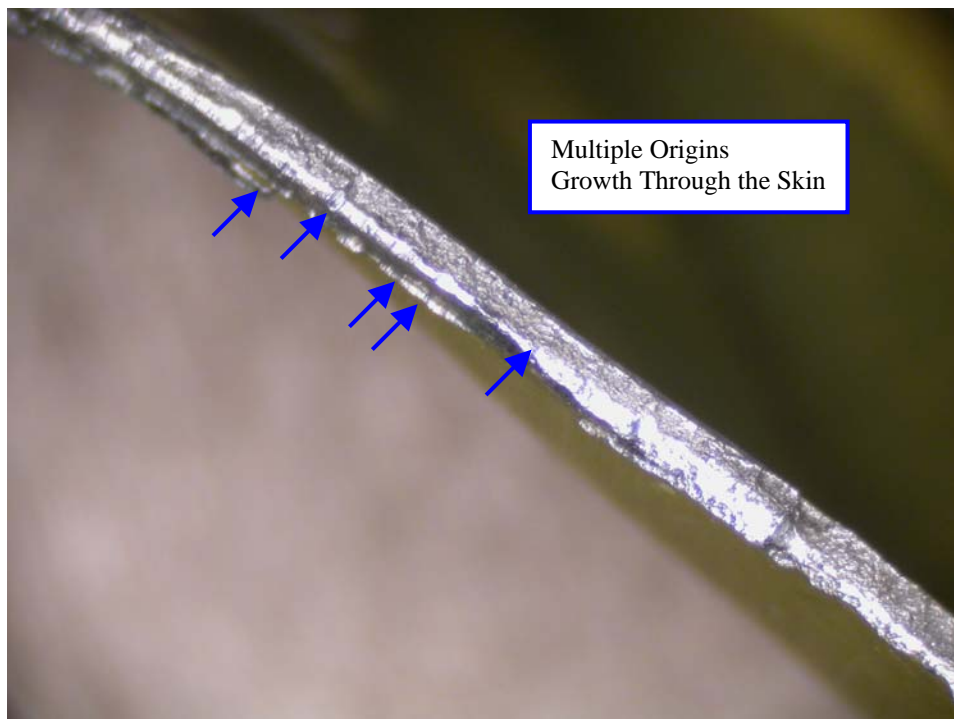


FIGURE 41. CRACK 24 FRACTURE FACE

### 2.3.2 Vertical and Horizontal Stabilizer Attachment Points.

Following the extraction and disassembly of the four areas of interest, a fluorescent liquid penetrant inspection was performed on the horizontal and vertical stabilizer attachment points in conjunction with the microscopic examination in an effort to find smaller cracks in the surrounding structure. Ten cracks were found on the vertical and horizontal stabilizer bulkheads. Figure 42 shows the location of crack 26 in the vertical stabilizer bulkhead top layer. Crack 26, shown in figure 43, had a total length of 1.4 inches, was through the thickness, and was caused solely by overload.

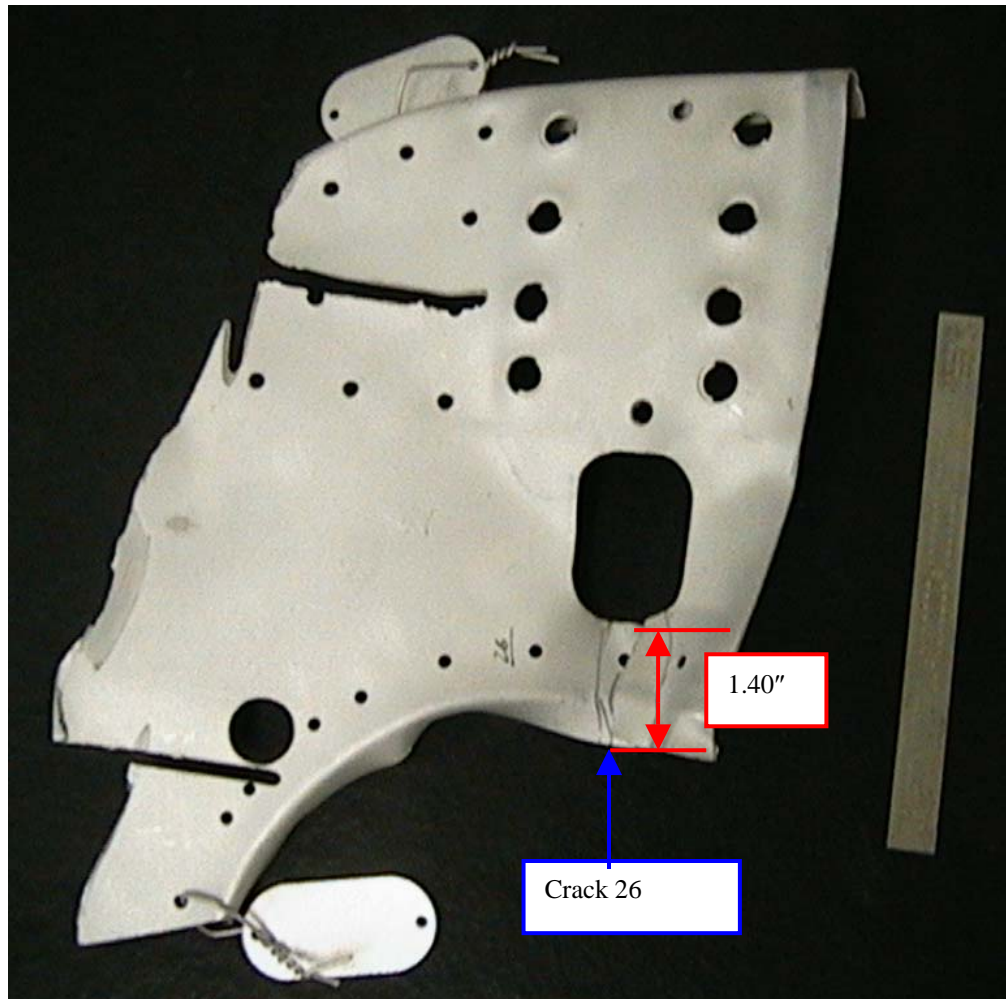


FIGURE 42. LOCATION OF CRACK 26 IN THE VERTICAL STABILIZER BULKHEAD TOP LAYER

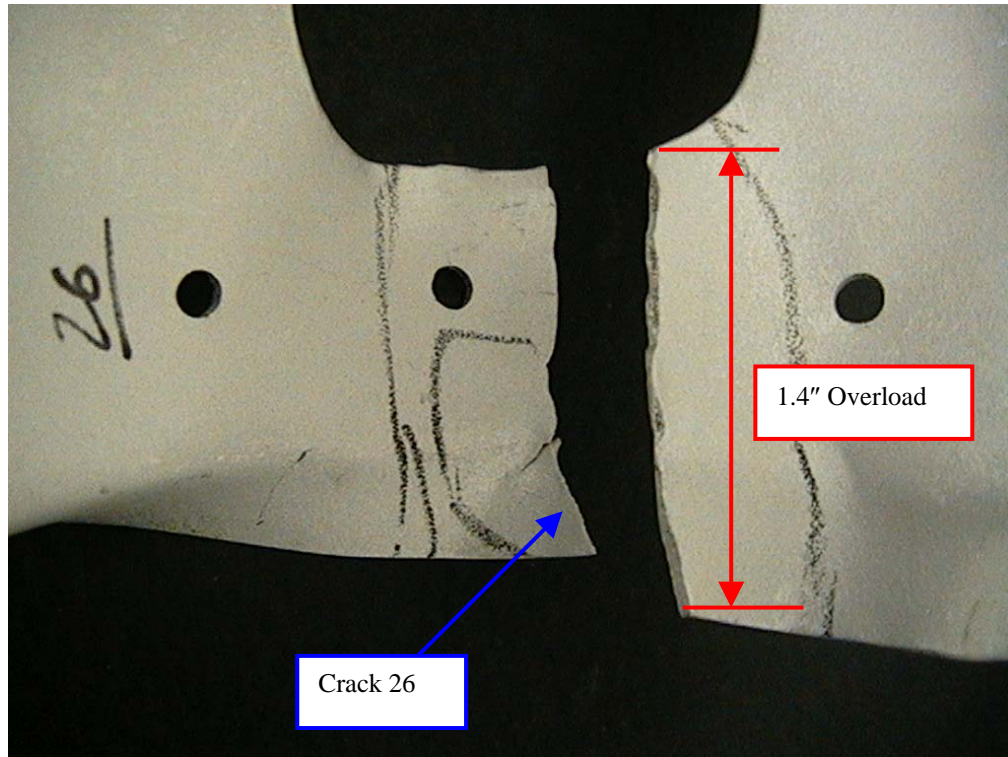


FIGURE 43. CRACK 26 IN THE VERTICAL STABILIZER BULKHEAD TOP LAYER

Figure 44 shows the locations of cracks 27 and 28 in the vertical stabilizer bulkhead middle layer. Crack 27, shown in figure 45, had a total length of 0.91 inch and was caused solely by overload, while crack 28 had a total length of 0.28 inch and was also caused by overload. Crack 28 was though the thickness and is shown in figure 46. Crack 28 is also shown in figure 47 during the fluorescent liquid penetrant inspection.



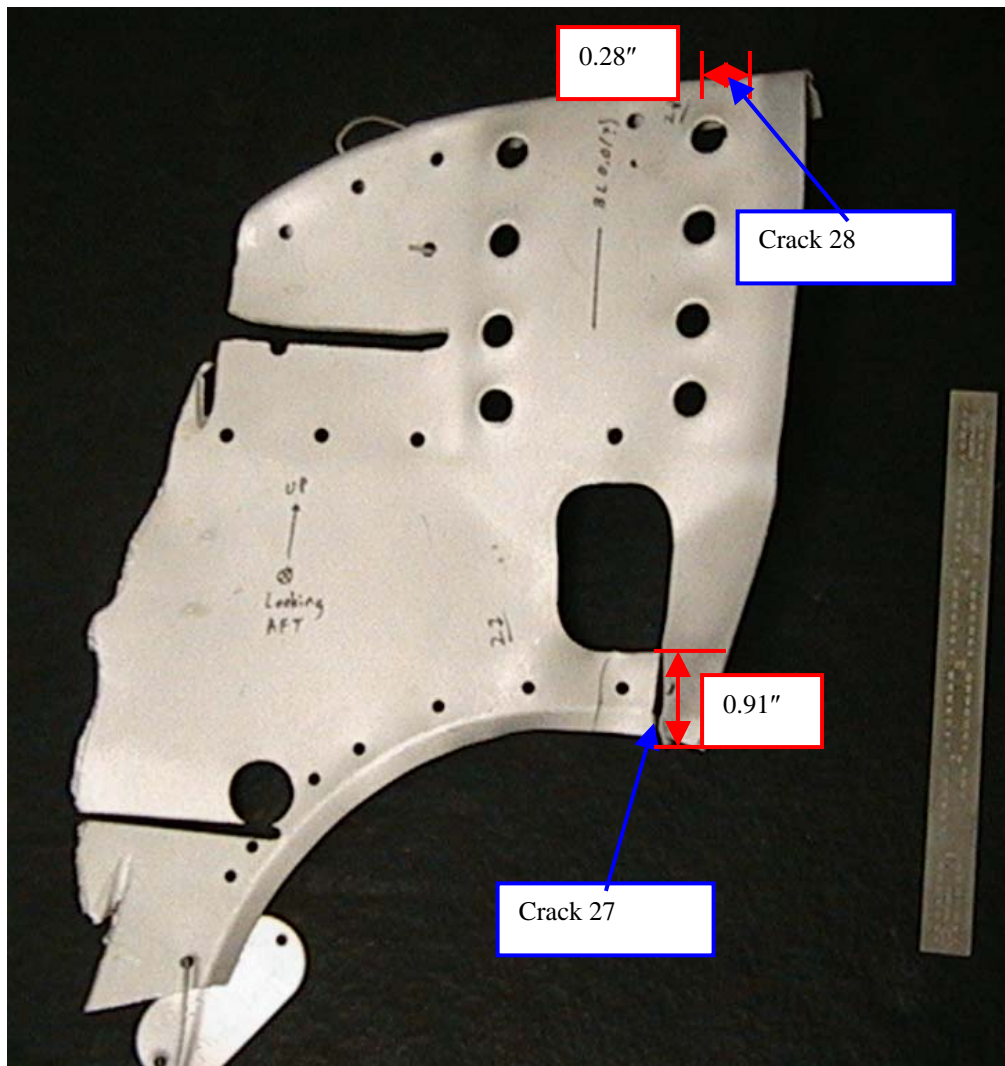


FIGURE 44. LOCATIONS OF CRACKS 27 AND 28 IN THE VERTICAL STABILIZER BULKHEAD MIDDLE LAYER

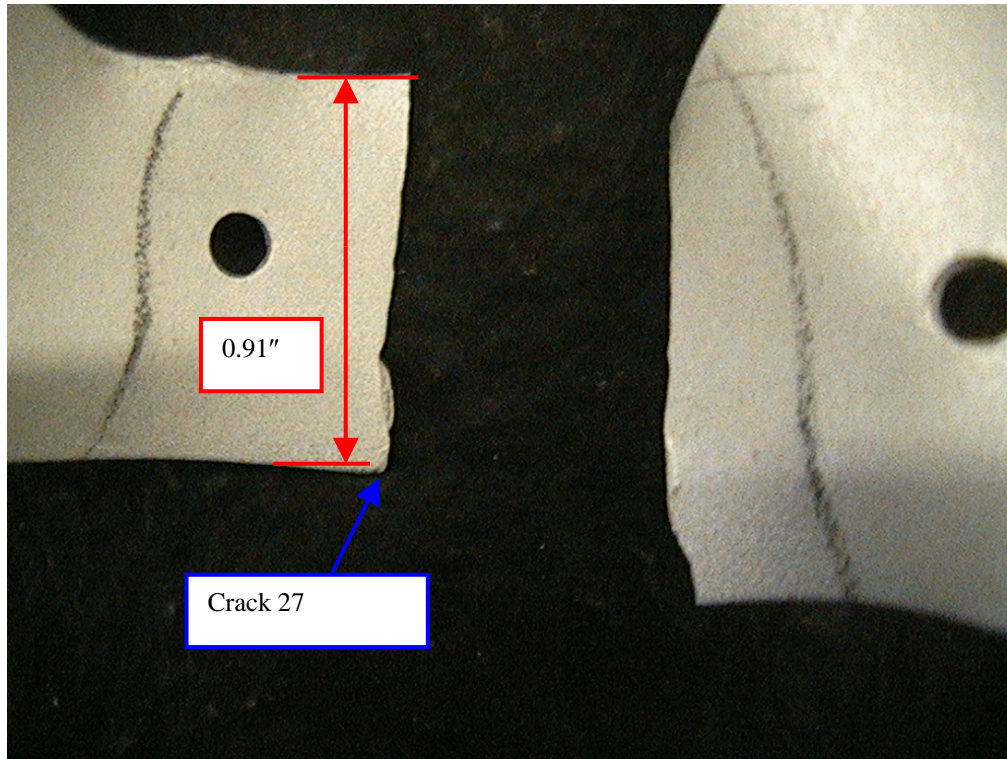


FIGURE 45. CRACK 27 IN THE VERTICAL STABILIZER BULKHEAD MIDDLE LAYER

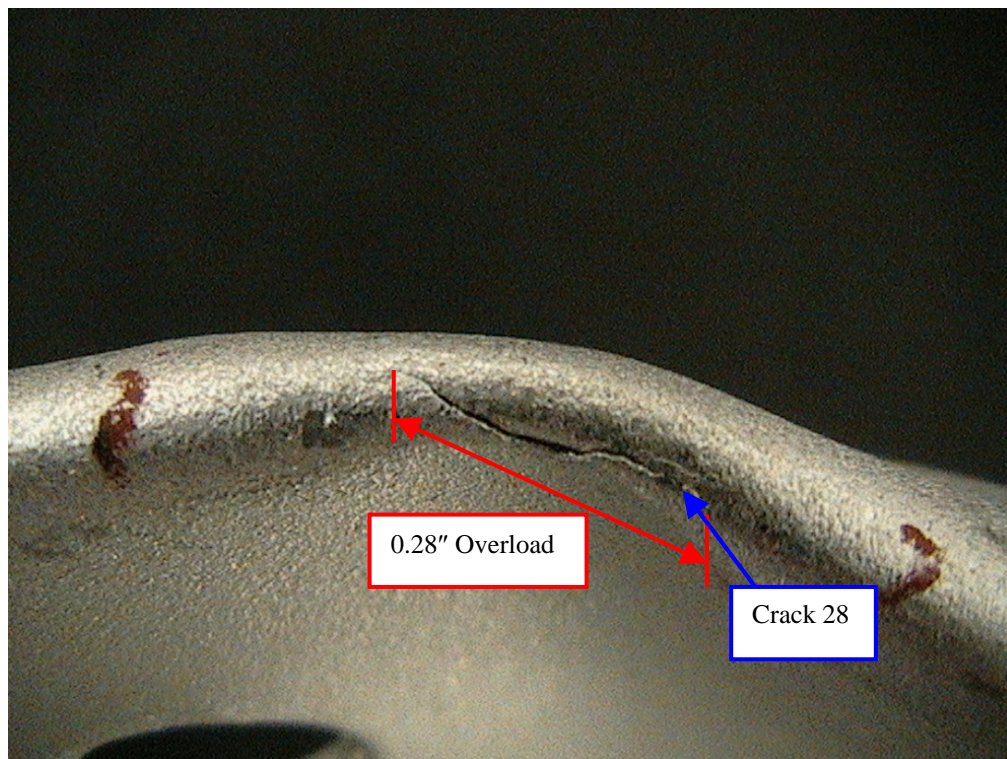


FIGURE 46. CRACK 28 IN THE VERTICAL STABILIZER BULKHEAD MIDDLE LAYER



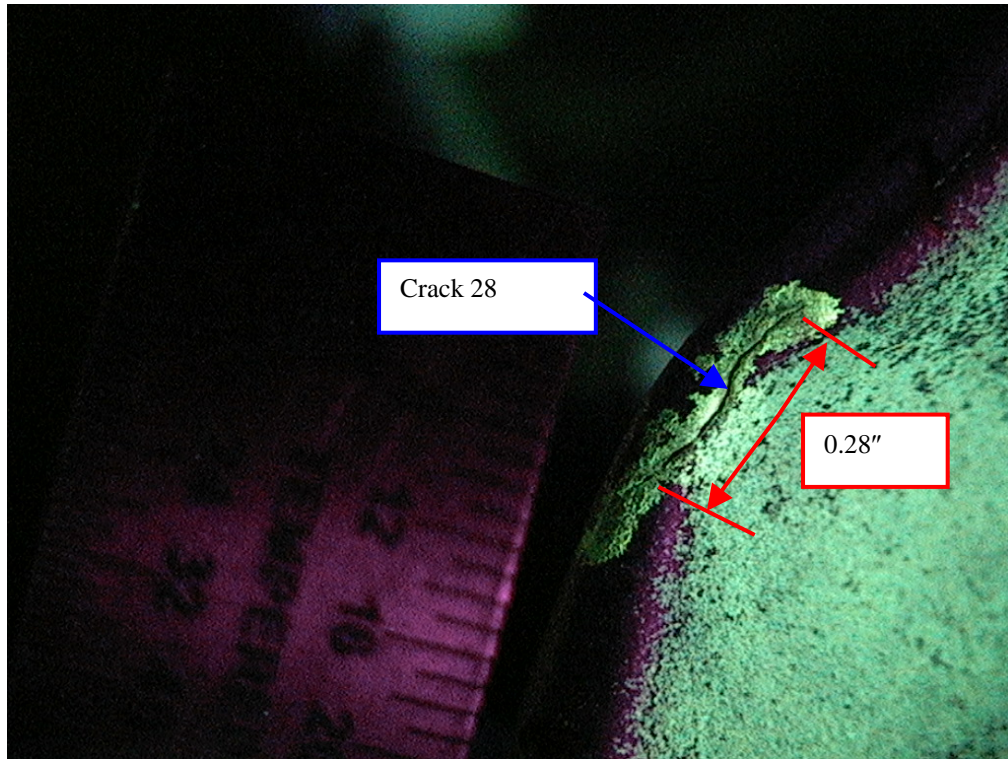


FIGURE 47. CRACK 28 IN THE VERTICAL STABILIZER BULKHEAD MIDDLE LAYER DURING THE FLUORESCENT LIQUID PENETRANT INSPECTION

Crack 29 was located on the vertical stabilizer bulkhead bottom layer and measured 0.50 inch. This crack, shown in figure 48, was caused solely by overload. Figure 49 shows crack 29 during the fluorescent liquid penetrant inspection process. Figure 50 shows the locations of cracks 30, 31, and 32 in the horizontal stabilizer bulkhead top layer. Figure 51 shows crack 30, which had a total length of 0.13 inch, was through the thickness, and was caused solely by overload. A picture of this crack under ultraviolet light is provided in figure 52. Crack 31, shown in figure 53, had a total length of 0.19 inch and was caused by overload. Figure 54 shows crack 31 under ultraviolet light during the fluorescent liquid penetrant inspections. Overload was also the only failure mechanism observed on crack 32, shown in figure 55. Crack 32 had a total length of 1.13 inch. Figure 56 shows the crack during the fluorescent liquid penetrant inspection process.



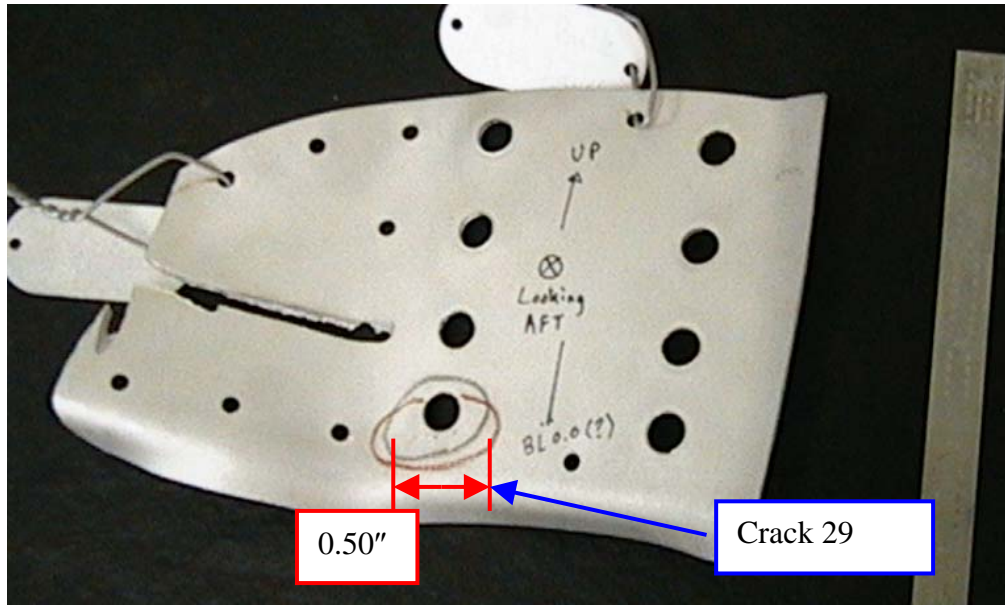


FIGURE 48. CRACK 29 IN THE VERTICAL STABILIZER BULKHEAD BOTTOM LAYER

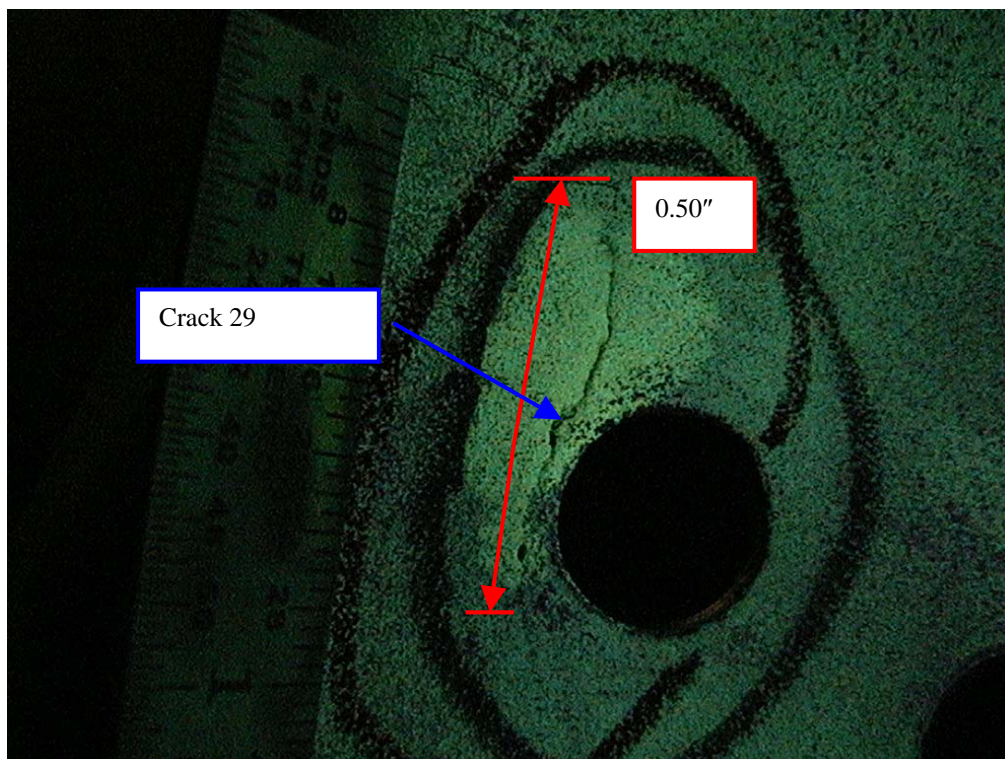


FIGURE 49. CRACK 29 IN THE VERTICAL STABILIZER BULKHEAD BOTTOM LAYER DURING THE FLUORESCENT LIQUID PENETRANT INSPECTION

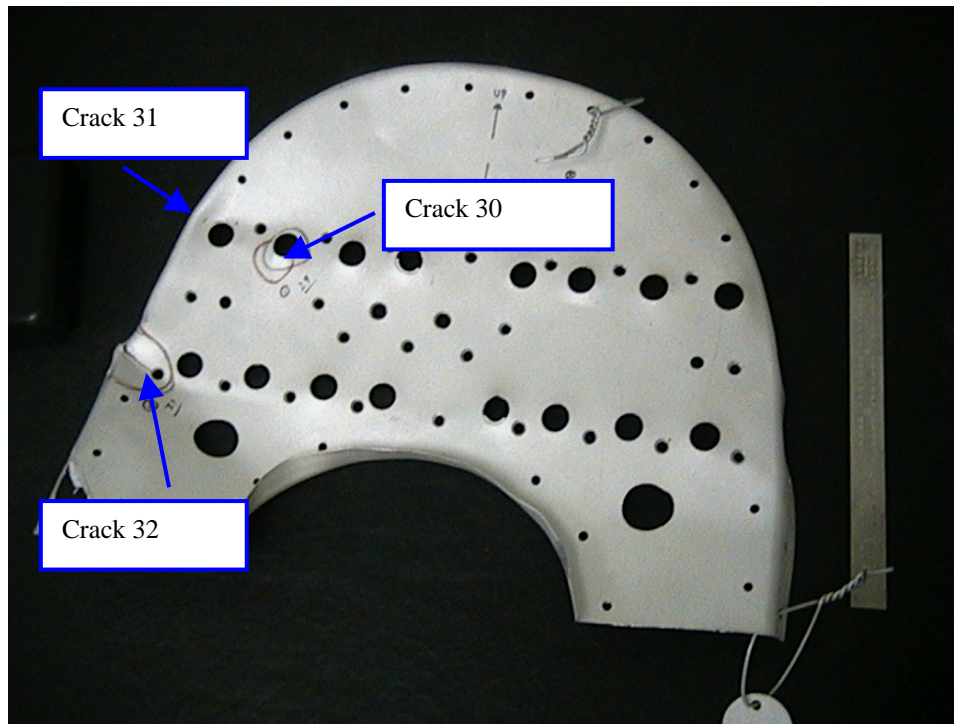


FIGURE 50. LOCATIONS OF CRACKS 30, 31, AND 32 IN THE HORIZONTAL STABILIZER BULKHEAD TOP LAYER

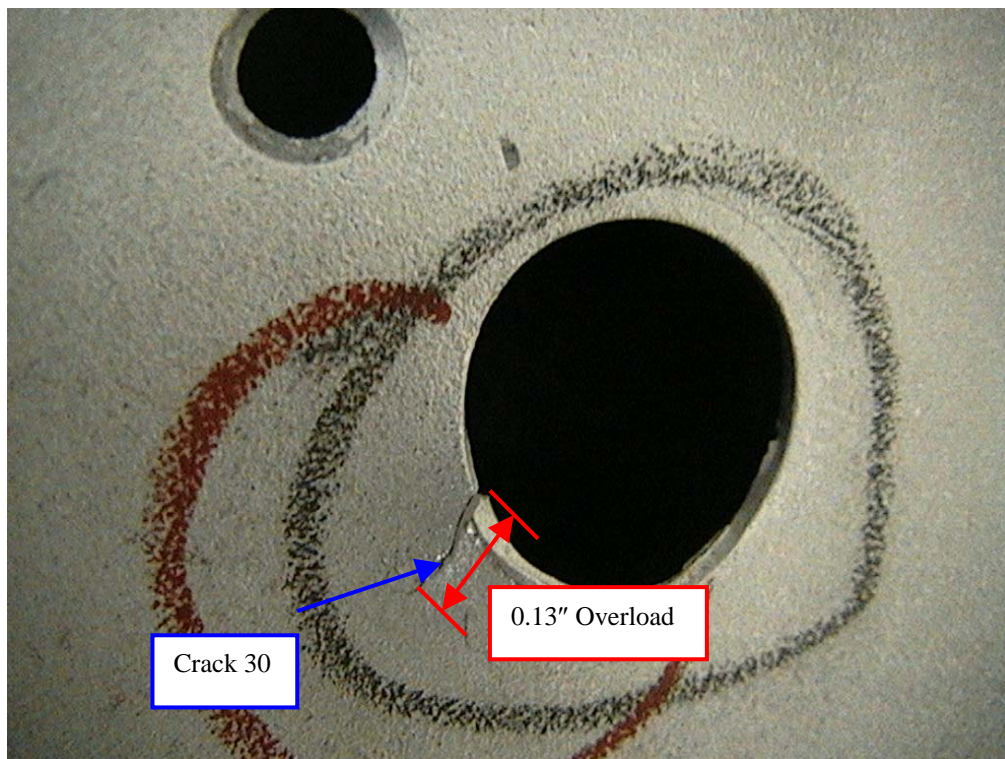


FIGURE 51. CRACK 30 IN THE HORIZONTAL STABILIZER BULKHEAD TOP LAYER



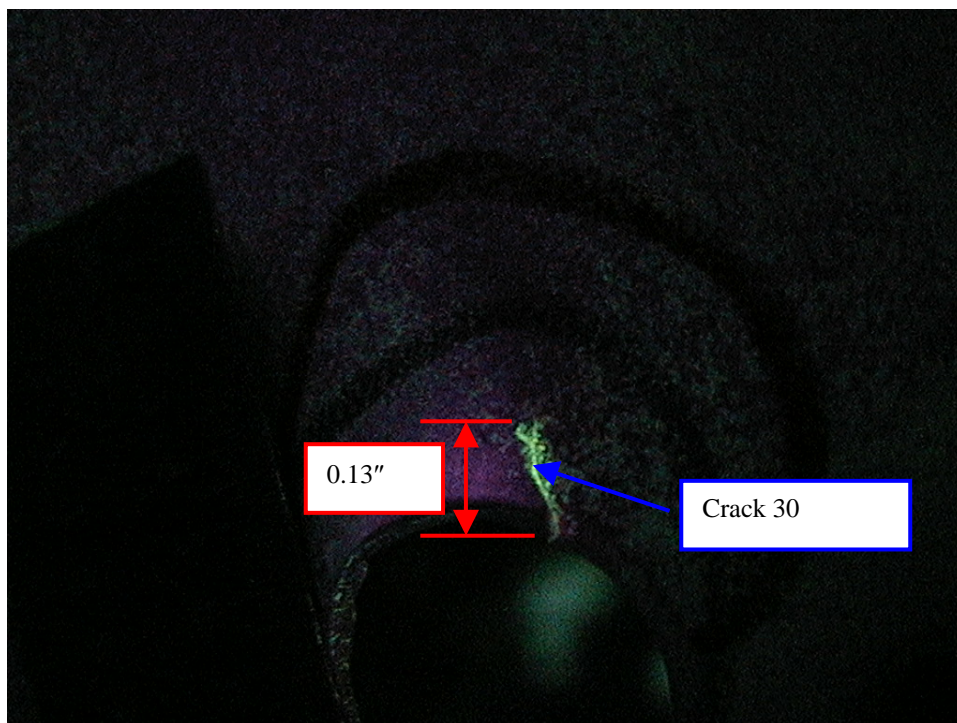


FIGURE 52. CRACK 30 IN THE HORIZONTAL STABILIZER BULKHEAD TOP LAYER UNDER ULTRAVIOLET LIGHT

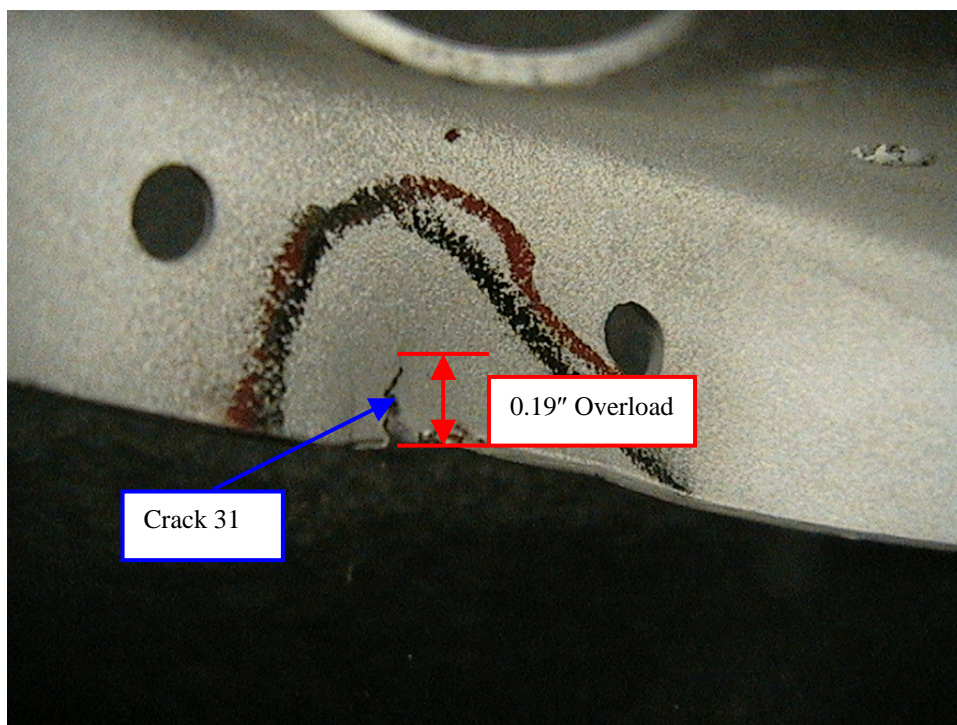


FIGURE 53. CRACK 31 IN THE HORIZONTAL STABILIZER BULKHEAD TOP LAYER

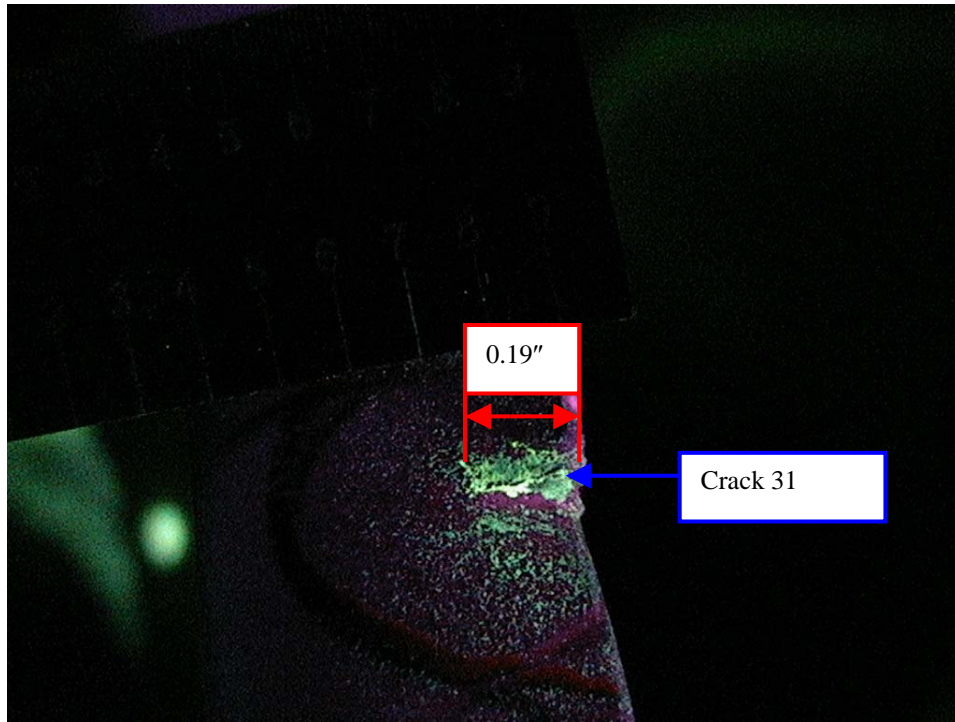


FIGURE 54. CRACK 31 IN THE HORIZONTAL STABILIZER BULKHEAD TOP LAYER DURING THE FLUORESCENT LIQUID PENETRANT INSPECTION

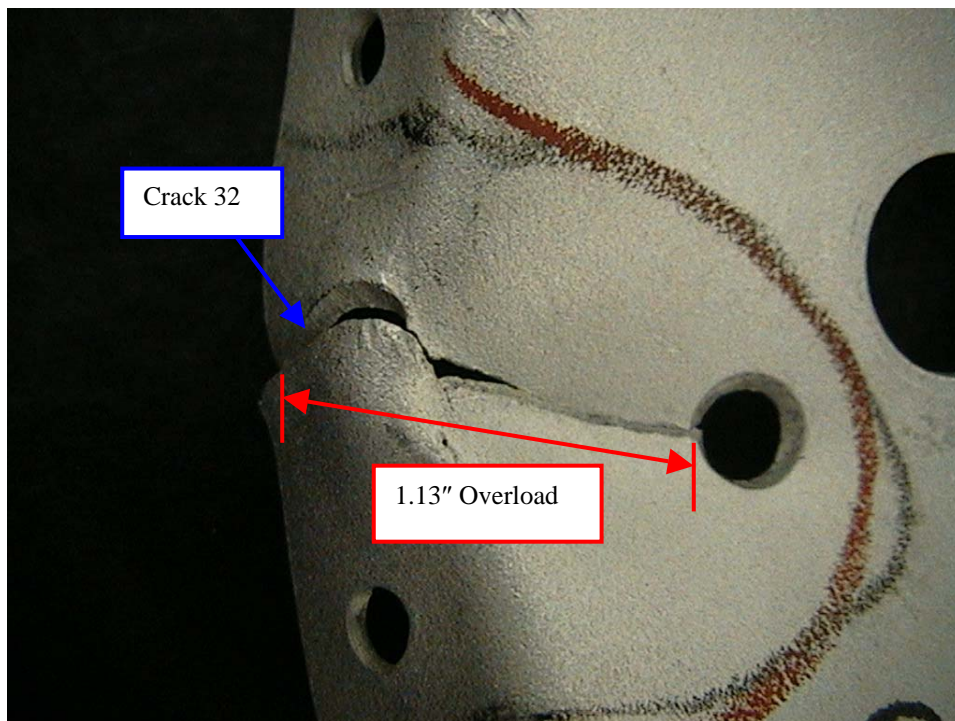


FIGURE 55. CRACK 32 IN THE HORIZONTAL STABILIZER BULKHEAD TOP LAYER



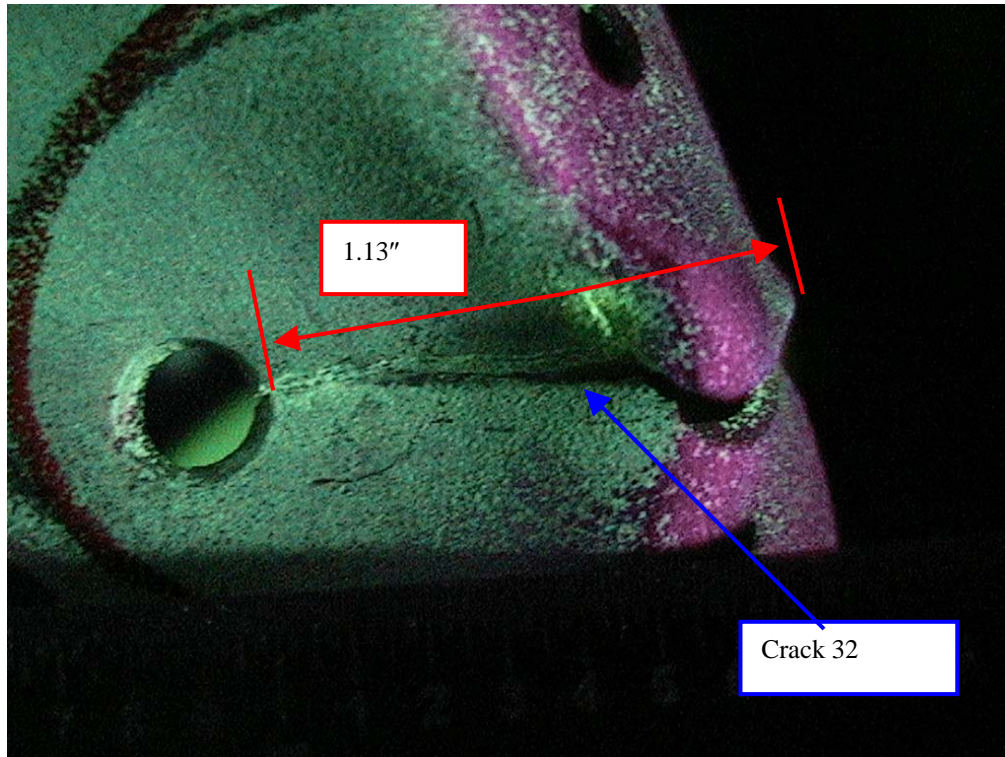


FIGURE 56. CRACK 32 IN THE HORIZONTAL STABILIZER BULKHEAD TOP LAYER UNDER ULTRAVIOLET LIGHT

The locations of cracks 33-35 in the horizontal stabilizer bulkhead middle layer are shown in figure 57. Crack 33, shown in figure 58, had a total length of 0.43 inch and was caused by overload, while figure 60 shows crack 34, which had a total length of 0.23 inch that was also caused solely by overload. Pictures taken during the fluorescent liquid penetrant inspections of cracks 33 and 34 are shown in figures 59 and 61, respectively. Figure 62 shows crack 35 with a total length of 0.62 inch. Figure 63 shows this crack under ultraviolet light during the fluorescent liquid penetrant inspections. The only failure mode observed with this crack was overload.



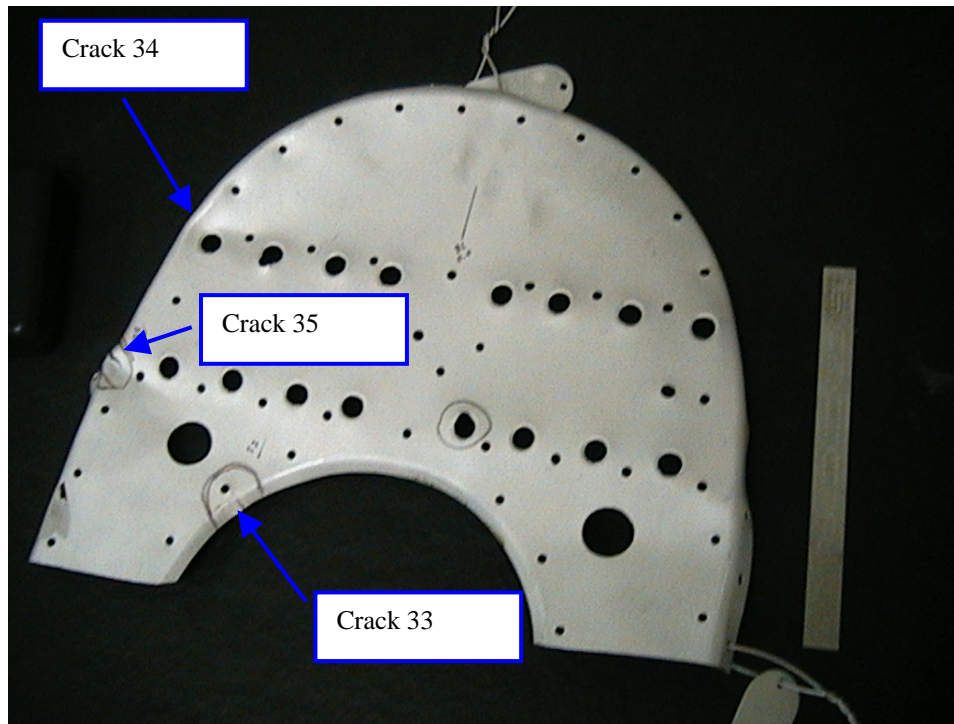


FIGURE 57. LOCATIONS OF CRACKS 33, 34, AND 35 IN THE HORIZONTAL STABILIZER BULKHEAD MIDDLE LAYER

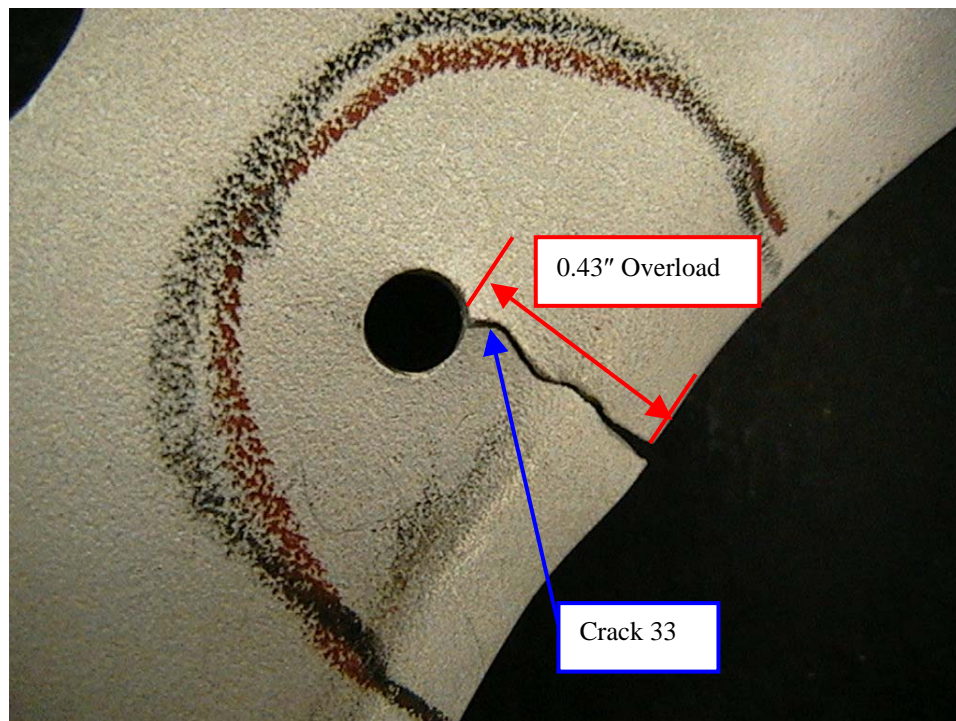


FIGURE 58. CRACK 33 IN THE HORIZONTAL STABILIZER BULKHEAD MIDDLE LAYER



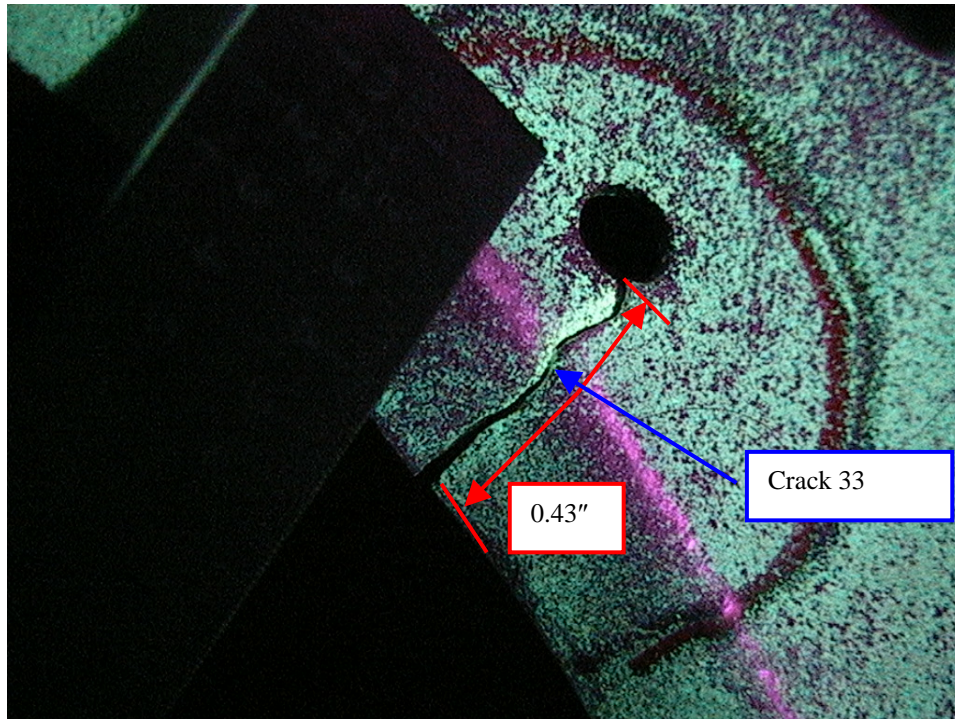


FIGURE 59. CRACK 33 IN THE HORIZONTAL STABILIZER BULKHEAD MIDDLE LAYER DURING THE FLUORESCENT LIQUID PENETRANT INSPECTION

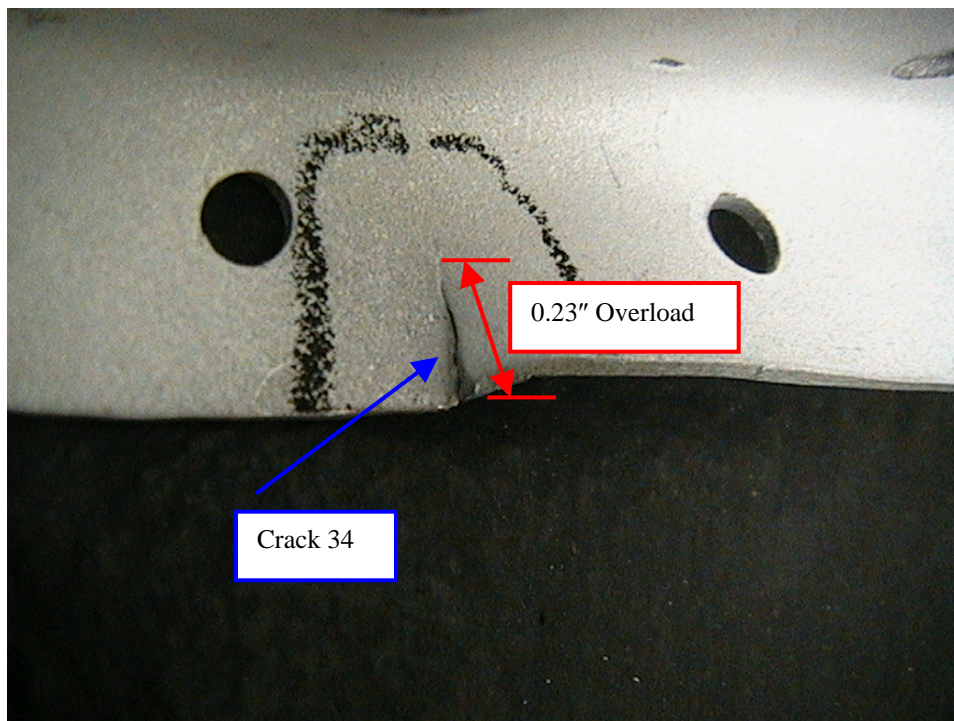


FIGURE 60. CRACK 34 IN THE HORIZONTAL STABILIZER BULKHEAD MIDDLE LAYER

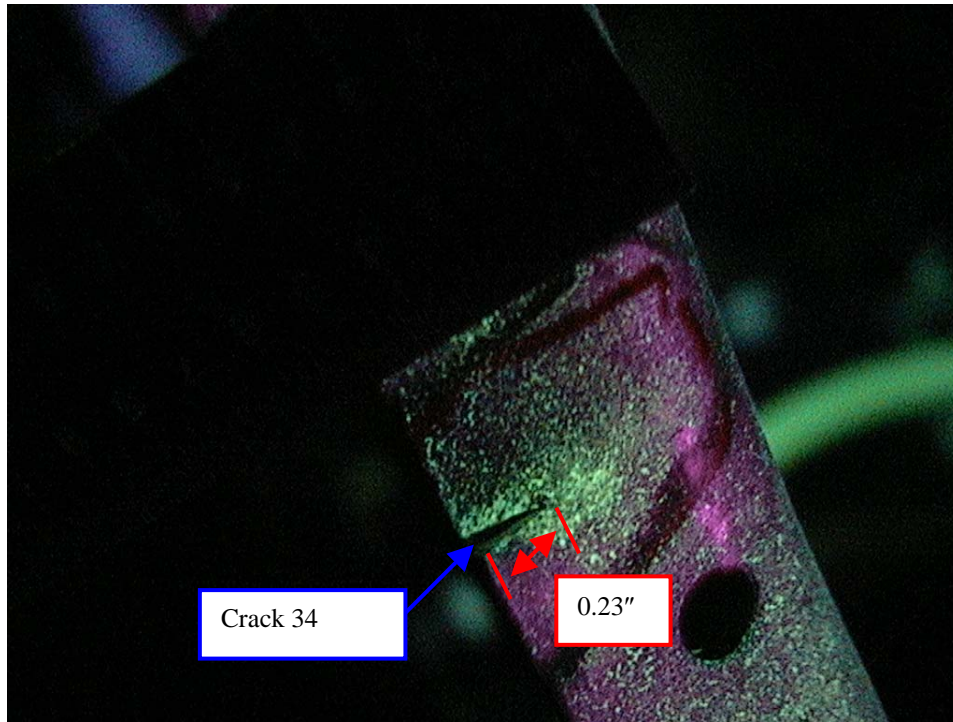


FIGURE 61. CRACK 34 IN THE HORIZONTAL STABILIZER BULKHEAD MIDDLE LAYER UNDER ULTRAVIOLET LIGHT

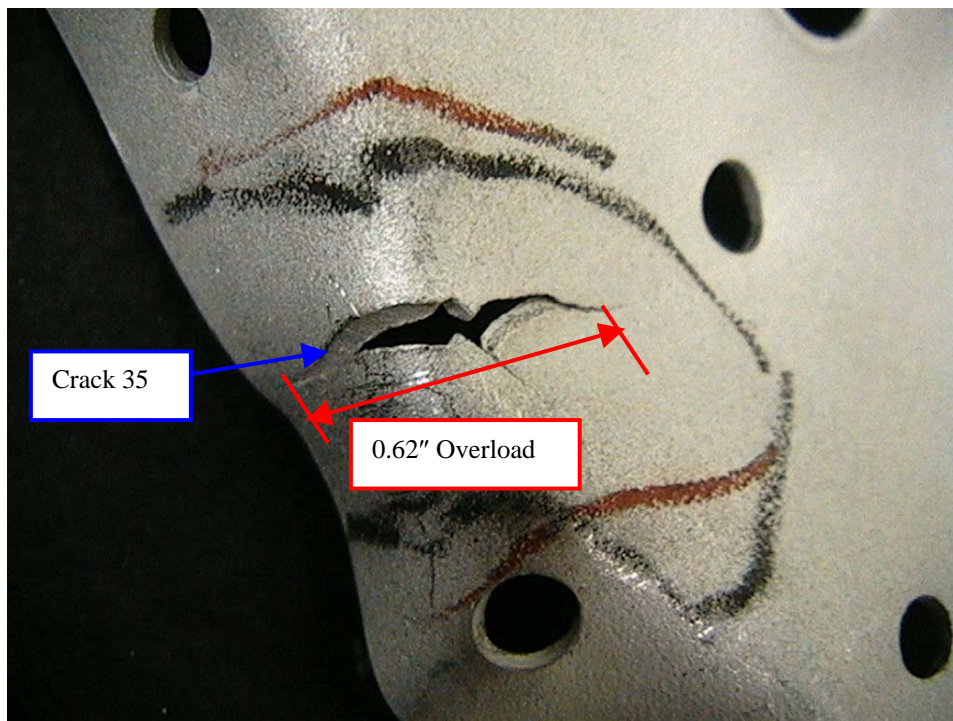


FIGURE 62. CRACK 35 IN THE HORIZONTAL STABILIZER BULKHEAD MIDDLE LAYER



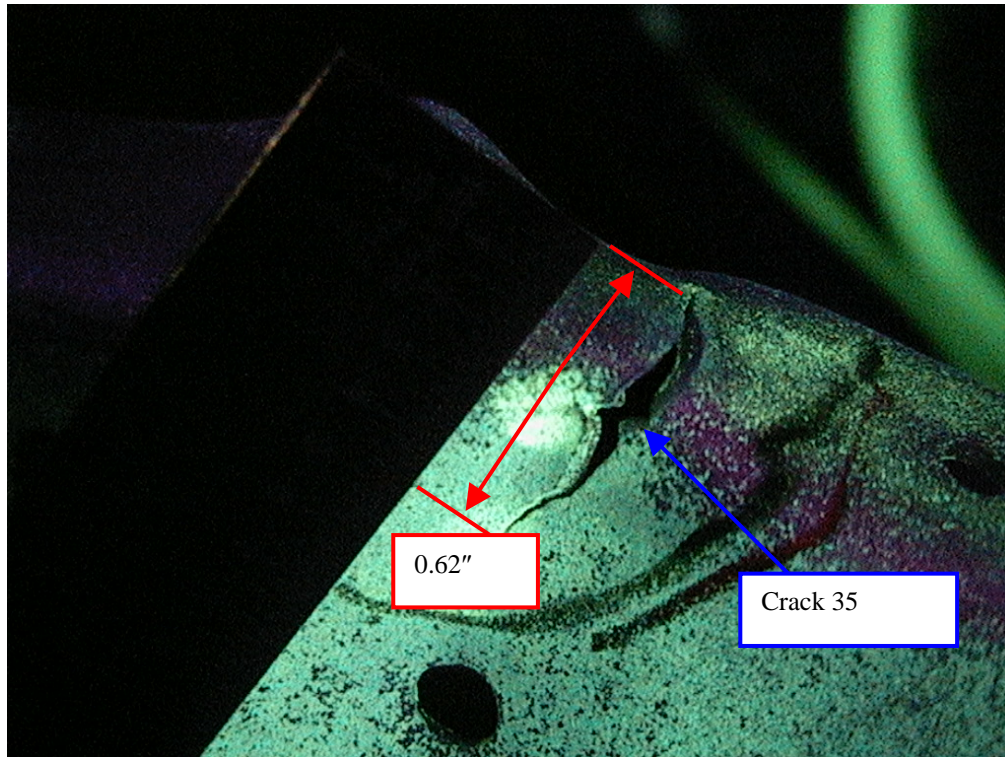


FIGURE 63. CRACK 35 IN THE HORIZONTAL STABILIZER BULKHEAD MIDDLE LAYER DURING THE FLUORESCENT LIQUID PENETRANT INSPECTION

### 2.3.3 Right Wing Rear Spar WS 66.

Two 1.187-inch cracks, cracks 36 and 37, were found on the right wing rear spar at WS 66. An overview of this area is provided in figure 64, while a detailed picture is shown in figure 65. The fracture face for crack 36 is shown in figure 66. The SEM fractograph of crack 36, shown in figure 67, shows metal smearing on the face, which masks all evidence of the failure mode. Figure 68 shows the fracture face of crack 37, while figure 69 provides the SEM fractograph. Like crack 36, crack 37 has a significant amount of metal smearing on the fracture face, which masks all evidence of the true failure mode. Therefore, the failure modes of cracks 36 and 37 could not be definitively determined due to smearing of the crack faces.



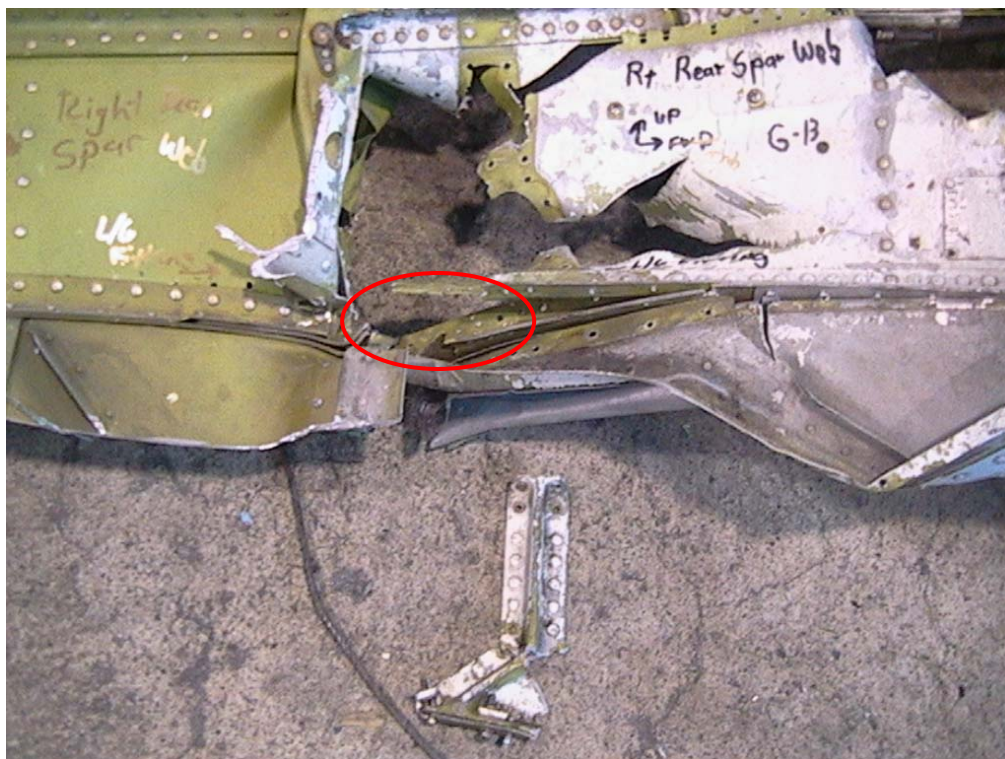


FIGURE 64. OVERVIEW OF CRACK LOCATIONS AT WS 66

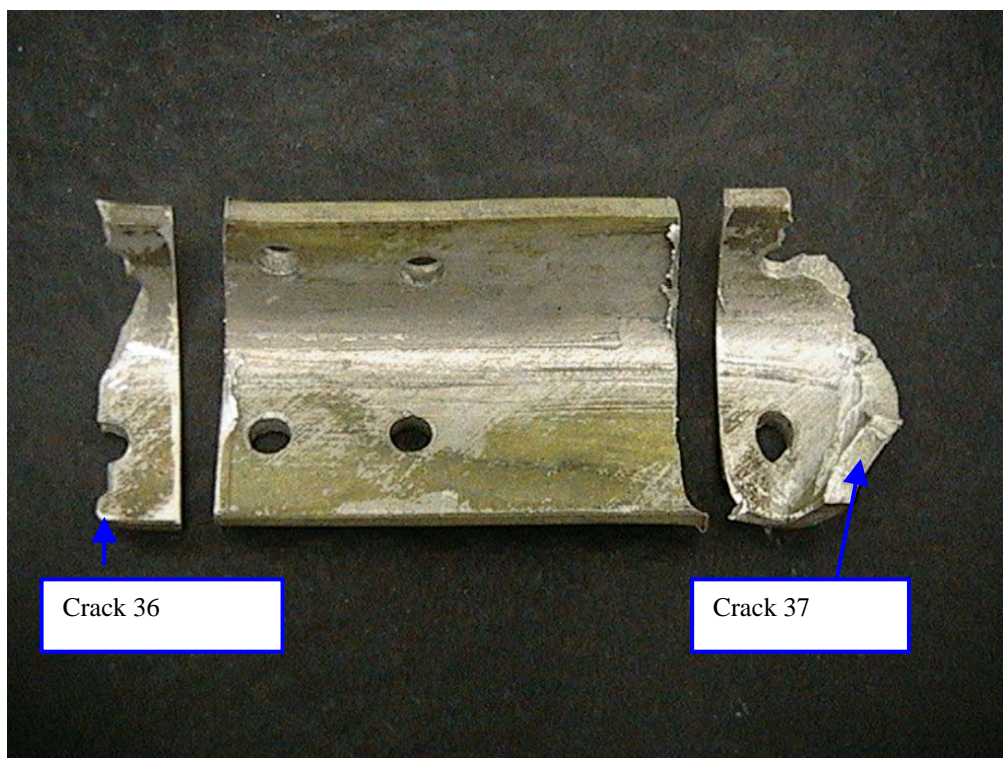


FIGURE 65. CRACKS 36 AND 37 ON RIGHT WING REAR SPAR WS 66



FIGURE 66. CRACK 36 FRACTURE FACE

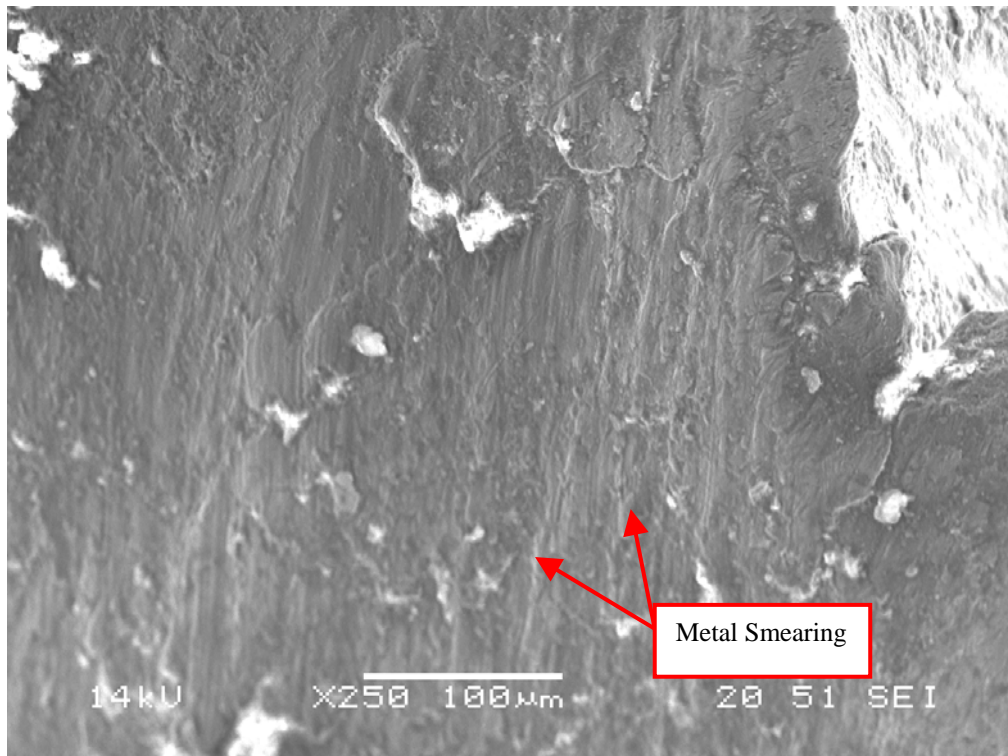


FIGURE 67. SURFACE FACE SEM FRACTOGRAPH OF CRACK 36





FIGURE 68. CRACK 37 FRACTURE FACE

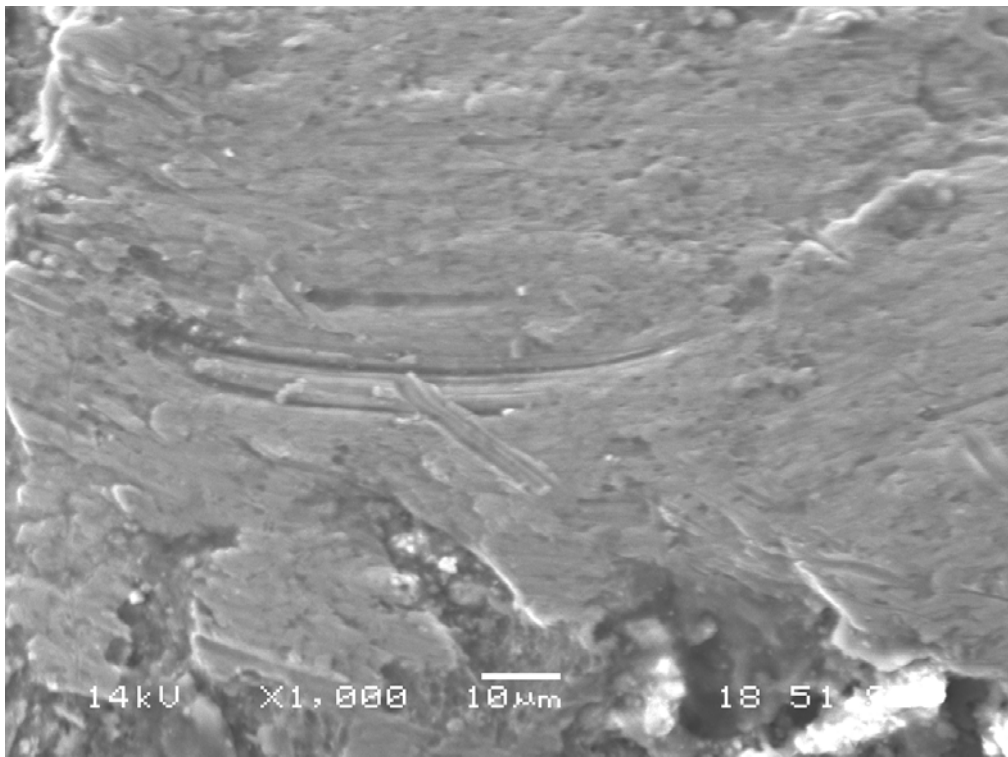


FIGURE 69. SURFACE FACE SEM FRACTOGRAPH OF CRACK 37

#### 2.3.4 Right Wing Rear Spar Bathtub Fitting.

Crack 38 found on the right wing rear spar lower bathtub fitting, shown in figure 70, was examined, and no evidence of fatigue was found. This crack measured 3.29 inches.

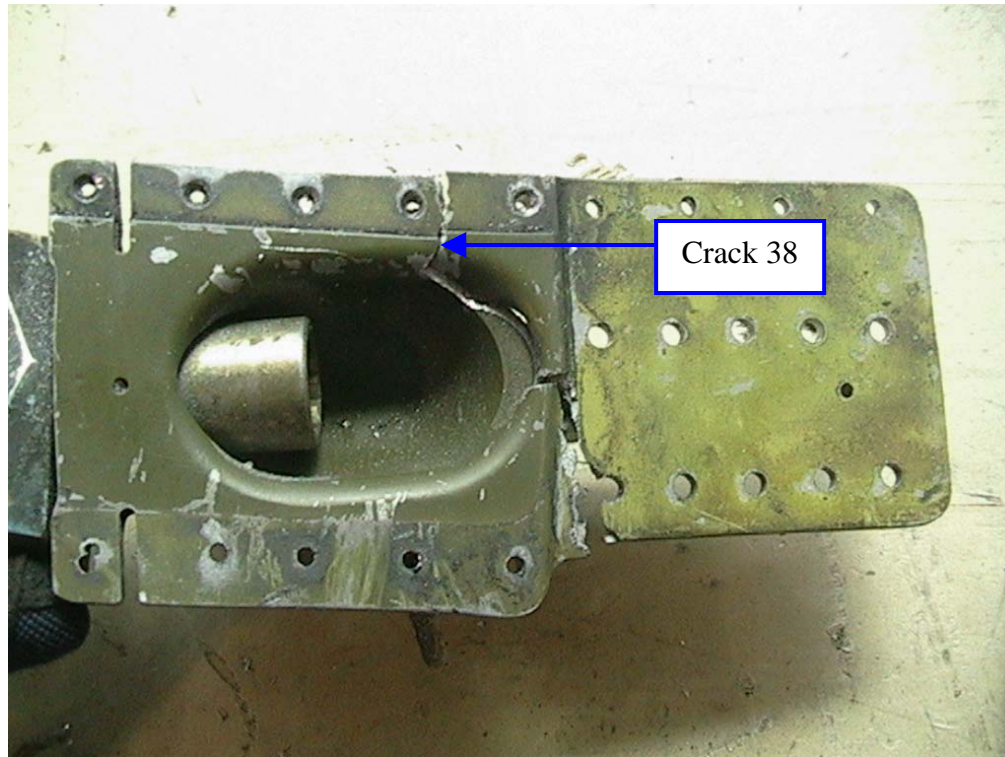


FIGURE 70. RIGHT WING REAR SPAR LOWER BATHTUB FITTING

### 3. SUMMARY OF FINDINGS.

The NIAR and the FAA performed a teardown evaluation of four areas of interest from the T-34A N141SW accident aircraft after it was released by the NTSB. The following four areas of interest were inspected for cracks and corrosion: the right wing front carry-through lower spar, horizontal and vertical stabilizer attachment points, right wing rear spar lower cap at WS 66, and right wing rear spar lower bathtub fitting. These areas were extracted from the aircraft wreckage and completely disassembled. Several areas were inspected with fluorescent liquid penetrant; all areas were microscopically examined; and most cracks were analyzed to determine failure mode.

During the destructive evaluation, 25 cracks were found on the right wing front carry-through lower spar, 10 cracks were located on the horizontal and vertical stabilizer attachment points, 2 cracks were identified on the right wing lower spar cap at WS 66, and 1 crack was observed on the right wing rear spar lower bathtub fitting.

Table 1 provides a summary of all cracks found during the teardown evaluation of the four areas of interest on the N141SW accident aircraft.



TABLE 1. SUMMARY OF FINDINGS FOR T-34A ACCIDENT AIRCRAFT

Part Description	Crack Number	Total Crack Length (Inches)	Fatigue Crack Length (Inches)
Right wing front carry-through Middle (-31) channel forward side	1	0.63	0.14
Right wing front carry-through Middle (-31) channel forward side	2	0.73	0.27
Right wing front carry-through Middle (-31) channel aft side	3	0.60	0.32
Right wing front carry-through Middle (-31) channel aft side	4	0.79	0.42
Right wing front carry-through Middle (-31) channel lower surface	5	0.09	0.08
Right wing front carry-through Middle (-31) channel lower surface	6	0.13	Not Opened <sup>2</sup>
Right wing front carry-through Outer (-33) channel forward side	7	0.15	Overload <sup>1</sup>
Right wing front carry-through Outer (-33) channel forward side	8	0.17	0.15
Right wing front carry-through Outer (-33) channel aft side	9	0.19	Not Opened <sup>2</sup>
Right wing front carry-through Outer (-33) channel aft side	10	0.34	0.27
Right wing front carry-through Outer (-33) channel lower surface	11	0.10	Not Opened <sup>2</sup>
Right wing front carry-through Outer (-33) channel lower surface	12	0.80	0.13
Right wing front carry-through Middle layer aft side web skin	13	0.31	0.05
Right wing front carry-through Middle layer aft side web skin	14	0.52	0.22
Right wing front carry-through Middle layer aft side web skin	15	0.26	Not Opened <sup>2</sup>
Right wing front carry-through Middle layer aft side web skin	16	1.12	Unknown <sup>3</sup>
Right wing front carry-through Middle layer aft side web skin	17	1.17	Unknown <sup>3</sup>
Right wing front carry-through Middle layer aft side web skin	18	0.53	0.53

TABLE 1. SUMMARY OF FINDINGS FOR T-34A ACCIDENT AIRCRAFT (Continued)

Part Description	Crack Number	Total Crack Length (Inches)	Fatigue Crack Length (Inches)
Right wing front carry-through Middle layer aft side web skin	19	0.20	0.20
Right wing front carry-through Middle layer aft side web skin	20	0.14	0.14
Right wing front carry-through Middle layer aft side web skin	21	0.09	0.09
Right wing front carry-through Middle layer aft side web skin	22	0.27	Overload <sup>1</sup>
Right wing front carry-through Middle layer forward side web skin	23	5.28	Overload <sup>1</sup>
Right wing front carry-through Middle layer forward side web skin	24	0.99	0.79
Right wing front carry-through Middle layer forward side web skin	25	0.21	0.18
Vertical stabilizer bulkhead top layer	26	1.40	Overload <sup>1</sup>
Vertical stabilizer bulkhead middle layer	27	0.91	Overload <sup>1</sup>
Vertical stabilizer bulkhead middle layer	28	0.28	Overload <sup>1</sup>
Vertical stabilizer bulkhead bottom layer	29	0.50	Overload <sup>1</sup>
Horizontal stabilizer bulkhead top layer	30	0.13	Overload <sup>1</sup>
Horizontal stabilizer bulkhead top layer	31	0.19	Overload <sup>1</sup>
Horizontal stabilizer bulkhead top layer	32	1.13	Overload <sup>1</sup>
Horizontal stabilizer bulkhead middle layer	33	0.43	Overload <sup>1</sup>
Horizontal stabilizer bulkhead middle layer	34	0.23	Overload <sup>1</sup>
Horizontal stabilizer bulkhead middle layer	35	0.62	Overload <sup>1</sup>
Right wing rear spar lower cap WS 66	36	1.187	Unknown <sup>3</sup>

TABLE 1. SUMMARY OF FINDINGS FOR T-34A ACCIDENT AIRCRAFT (Continued)

Part Description	Crack Number	Total Crack Length (Inches)	Fatigue Crack Length (Inches)
Right wing rear spar lower cap WS 66	37	1.187	Unknown <sup>3</sup>
Right wing rear spar lower bathtub fitting	38	3.29	Unknown <sup>3</sup>

Notes:

<sup>1</sup> Failure was caused solely by overload.

<sup>2</sup> Crack was not opened for examination due either to its proximity and similarity to other cracks that were examined as part of this effort or to its location on the part prohibiting examination of the fracture surface.

<sup>3</sup> Cause of failure was unknown due to damage and/or metal smearing of the fracture face.